Table IV Most common related AEs during the entire SCIG treatment period (SCIG wash-in/wash-out and SCIG efficacy periods) by preferred term (AT)

Preferred term	At least possibly related		At least possibly related and temporally associated events (72 h)	
	Number of patients (%)	Number of events (rate per infusion)	Number of patients (%)	Number of events (rate per infusion)
Total number of patients or infusions	25	584	25	584
Any preferred term	21 (84.0)	175 (0.300)	21 (84.0)	170 (0.291)
Local reactions[a]	20 (80.0)	160 (0.274)	20 (80.0)	156 (0.267)
Skin and subcutaneous tissue disorders	2 (8.0)	9 (0.015)	2 (8.0)	9 (0.015)
Gastrointestinal disorders	1 (4.0)	1 (0.002)	1 (4.0)	1 (0.002)
Investigations	1 (4.0)	1 (0.002)	0 (0.0)	0 (0.000)
Vascular disorders	1 (4.0)	1 (0.002)	1 (4.0)	1 (0.002)

[a] Based on 16 MedDRA preferred terms

AE adverse event, *AT* all treated data set, *SCIG* subcutaneous immunoglobulin

was considered by the investigator unrelated to study drug. A 22-year-old male with XLA experienced bacterial infection that was reported as an SAE because of the necessity of hospitalization. The patient was treated with antibacterials and the infection resolved after 15 days. This infection was not considered an SBI, as it did not meet the pre-specified US FDA criteria. No SAEs were reported during the IVIG treatment period.

There were no deaths or AEs resulting in discontinuation of treatment in this study.

Local Reactions

Local tolerability of 85.4 % of SCIG infusions was assessed by the patients as "very good" or "good". In no case was the local tolerability assessed as "poor".

AEs of local reactions occurred in 20 patients (80.0 %), with an overall rate of 0.277 events per infusion. Almost all local reactions (97.5 %) were temporally associated with SCIG infusion. The rate of local reactions decreased over time from 0.389 events per infusion during the SCIG wash-in/wash-out period to 0.163 events per infusion during the SCIG efficacy period. The overall rate of local reactions related to home-based infusions during the efficacy period was comparable with that related to infusions at investigational site (0.178 events per infusion versus 0.120 events per infusion, respectively).

Vital Signs, Laboratory Parameters, and Viral Safety

No consistent or clinically relevant changes in vital signs were reported in this study.

Median values and ranges of hematology, blood chemistry, and urinalysis did not show any relevant changes over time.

Viral safety screening for HIV-1, HIV-2, HCV, and HBV found no positive viral markers at either baseline or 12–17 weeks following the final SCIG infusion.

Discussion

Primary efficacy analysis of this study demonstrated that IgPro20 administered by the subcutaneous route in uniform weekly doses was an effective treatment in both adult and pediatric Japanese patients with PID. A dose-equivalent switch to SCIG 20 % was effective in maintaining total serum IgG trough levels equal to or above those achieved on the previous IVIG therapy (Fig. 3). The annualized rate of infection during the SCIG efficacy period (2.98 infections/patient/year) was in line with that observed in previous studies in Europe and in the US (2.76–5.18 infections/patient/year), as were the number of days missed from school/work/daycare and days spent in hospital [6, 7, 12]. The mean weekly dose of IgPro20 during the SCIG efficacy period was lower in the Japanese population than that seen in Europe and, in particular, the US [6, 7], probably due to the specifics of local treatment practices including limits on maximum dose allowed per patient.

This is the first prospective study of SCIG to incorporate a mandatory IVIG treatment period into the trial design, allowing for a more stringent comparison of SCIG and IVIG treatments than previous IgPro20 studies. As all patients had received at least 3 IVIG infusions at a stable dose before enrolling in the study, their IgG levels were expected to be at steady state by the end of the mandatory IVIG period. A 12-week SCIG wash-in/wash-out period ensured that the IVIG treatment did not affect serum IgG trough levels during the steady state SCIG efficacy period. SCIG dose adjustments during the wash-in/wash-out period were allowed, but were unlikely to affect the outcome of the study, as the minimal target serum IgG trough level (5.0 g/L) was lower than that achieved during the IVIG treatment period (6.53 g/L).

The male/female imbalance in the patient demographics can be explained by a large share of XLA patients in the study population. Of interest, this subgroup included one well-documented case of XLA in a female patient [17].

Higher rates of antibiotic use in this study compared with the same outcome in SCIG studies conducted outside Japan are likely associated with generally higher administration of antibiotics in Japan [18–20].

IgPro20 was well tolerated. No SAEs related to its administration were reported during the study. One SAE (bacterial infection; etiologic agent not identified) of moderate severity reported during the SCIG efficacy period occurred due to accidental infection and was considered unrelated to the study drug.

The overall incidence of AEs including local reactions during the SCIG wash-in/wash-out and SCIG efficacy periods (0.461 AEs per patient/year affecting 96 % of patients) was comparable with the overall AE rates in other SCIG studies in Europe and in the US (0.288–0.773 AEs per patient/year affecting 98–100 % of patients) [6, 7]. Mild or moderate local reactions (swelling, soreness, redness, and induration) are generally expected when relatively large volumes of IgG are infused by the subcutaneous route. The overall rates of local reactions reported in this study were in line with previous SCIG studies [6, 7, 11, 12].

Conclusions

Weekly SCIG treatment with Hizentra® was effective in pediatric and adult Japanese patients with PID requiring IgG replacement therapy. The treatment was well tolerated and demonstrated a highly favorable risk-benefit profile.

Acknowledgments The authors thank Dr Alphonse Hubsch for critical review of the manuscript. We also acknowledge the editorial assistance of Dr Alexey Veligodskiy from PHOCUS Services Ltd, a member of the Fishawack Group of Companies, supported by CSL Behring.

This study was supported by CSL Behring AG, Berne, Switzerland.

References

1. Al-Herz W, Bousfiha A, Casanova JL, Chapel H, Conley ME, Cunningham-Rundles C, et al. Primary immunodeficiency diseases: an update on the classification from the international union of immunological societies expert committee for primary immunodeficiency. Front Immunol. 2011;2:54.
2. Notarangelo L, Casanova JL, Fischer A, Puck J, Rosen F, Seger R, et al. Primary immunodeficiency diseases: an update. J Allergy Clin Immunol. 2004;114:677–87.
3. Buckley RH, Schiff RI. The use of intravenous immune globulin in immunodeficiency diseases. N Engl J Med. 1991;325:110–7.
4. Ishimura M, Takada H, Doi T, Imai K, Sasahara Y, Kanegane H, et al. Nationwide survey of patients with primary immunodeficiency diseases in Japan. J Clin Immunol. 2011;31:968–76.
5. Boyle JM, Buckley RH. Population prevalence of diagnosed primary immunodeficiency diseases in the United States. J Clin Immunol. 2007;27:497–502.
6. Hagan JB, Fasano MB, Spector S, Wasserman RL, Melamed I, Rojavin MA, et al. Efficacy and safety of a new 20 % immunoglobulin preparation for subcutaneous administration, IgPro20, in patients with primary immunodeficiency. J Clin Immunol. 2010;30:734–45.
7. Jolles S, Bernatowska E, de Gracia J, Borte M, Cristea V, Peter HH, et al. Efficacy and safety of Hizentra® in patients with primary immunodeficiency after a dose-equivalent switch from intravenous or subcutaneous replacement therapy. Clin Immunol. 2011;141:90–102.
8. Maarschalk-Ellerbroek LJ, Hoepelman IM, Ellerbroek PM. Immunoglobulin treatment in primary antibody deficiency. Int J Antimicrob Agents. 2011;37:396–404.
9. Ochs HD, Hitzig WH. History of primary immunodeficiency diseases. Curr Opin Allergy Clin Immunol. 2012;12:577–87.
10. Bonilla FA. Pharmacokinetics of immunoglobulin administered via intravenous or subcutaneous routes. Immunol Allergy Clin N Am. 2008;28:803–19.
11. Ochs HD, Gupta S, Kiessling P, Nicolay U, Berger M, Subcutaneous IgG Study Group. Safety and efficacy of self-administered subcutaneous immunoglobulin in patients with primary immunodeficiency diseases. J Clin Immunol. 2006;26:265–73.
12. Borte M, Pac M, Serban M, Gonzalez-Quevedo T, Grimbacher B, Jolles S, et al. Efficacy and safety of Hizentra®, a new 20 % immunoglobulin preparation for subcutaneous administration, in pediatric patients with primary immunodeficiency. J Clin Immunol. 2011;31:752–61.
13. Berger M, Rojavin M, Kiessling P, Zenker O. Pharmacokinetics of subcutaneous immunoglobulin and their use in dosing of replacement therapy in patients with primary immunodeficiencies. Clin Immunol. 2011;139:133–41.
14. Wasserman RL, Melamed I, Nelson Jr RP, Knutsen AP, Fasano MB, Stein MR, et al. Pharmacokinetics of subcutaneous IgPro20 in patients with primary immunodeficiency. Clin Pharmacokinet. 2011;50:405–14.
15. Conley ME, Notarangelo LD, Etzioni A. Diagnostic criteria for primary immunodeficiencies. Representing PAGID (Pan-American Group for Immunodeficiency) and ESID (European Society for Immunodeficiencies). Clin Immunol. 1999;93:190–7.
16. U.S. FDA. FDA Guidance for industry: safety, efficacy, and pharmacokinetic studies to support marketing of immune globulin intravenous (human) as replacement therapy for primary humoral immunodeficiency. 2008. http://www.fda.gov/downloads/BiologicsBloodVaccines/GuidanceComplianceRegulatoryInformation/Guidances/Blood/ucm078526.pdf 2008. Accessed 29 Jan 2013.
17. Takada H, Kanegane H, Nomura A, Yamamoto K, Ihara K, Takahashi Y, et al. Female agammaglobulinemia due to the Bruton tyrosine kinase deficiency caused by extremely skewed X-chromosome inactivation. Blood. 2004;103:185–7.
18. Kumazawa J, Yagisawa M. The history of antibiotics: the Japanese story. J Infect Chemother. 2002;8:125–33.
19. Sekimoto M, Imanaka Y, Evans E, Ishizaki T, Hirose M, Hayashida K, et al. Practice variation in perioperative antibiotic use in Japan. Int J Qual Health Care. 2004;16:367–73.
20. Ariyanchira S. Antibiotic resistance and antibiotic technologies: global markets. Market research report PHM025B. 2009. http://www.bccresearch.com/market-research/pharmaceuticals/antibiotic-resistance-technologies-phm025b.html. Accessed 29 Jan 2013.

RHEUMATOLOGY

Rheumatology 2014;53:1783–1787
doi:10.1093/rheumatology/keu180
Advance Access publication 11 May 2014

Concise report

Early progression of atherosclerosis in children with chronic infantile neurological cutaneous and articular syndrome

Kenichiro Yamamura[1], Hidetoshi Takada[1], Kiyoshi Uike[1], Yasutaka Nakashima[1], Yuichiro Hirata[1], Hazumu Nagata[1], Tomohito Takimoto[1], Masataka Ishimura[1], Eiji Morihana[1], Shouichi Ohga[2] and Toshiro Hara[1]

Abstract

Objective. Chronic inflammation plays a key role in the development of atherosclerosis. Early progression of atherosclerosis has been reported in patients with RA. Cryopyrin-associated periodic syndromes (CAPS) are autosomal dominant autoinflammatory disorders caused by heterozygous *NLRP3* gene mutations. Chronic infantile neurological cutaneous and articular (CINCA) syndrome is the most severe form of CAPS and patients display early onset of rash, fever, uveitis and joint manifestations. However, there has been no previous report on atherosclerosis in patients with CAPS. The objective of this study is to assess the development of atherosclerosis in patients with CINCA syndrome.

Methods. Intima–media thickness (IMT) of the carotid arteries, stiffness parameter β, ankle brachial index (ABI) and pressure wave velocity (PWV) were evaluated by ultrasonography in 3 patients with CINCA syndrome [mean age 9.0 years (S.D. 5.3)] and 19 age-matched healthy controls [9.3 years (S.D. 4.3)].

Results. The levels of carotid IMT, stiffness parameter β and PWV in CINCA syndrome patients were significantly higher than those in healthy controls [0.51 mm (S.D. 0.05) *vs* 0.44 (0.04), $P = 0.0021$; 6.1 (S.D. 1.7) *vs* 3.9 (1.0), $P = 0.0018$; 1203 cm/s (S.D. 328) *vs* 855 (114), $P = 0.017$, respectively].

Conclusion. Patients with CINCA syndrome showed signs of atherosclerosis from their early childhood. The results of this study emphasize the importance of chronic inflammation in the development of atherosclerosis. Further analysis on atherosclerosis in young patients with CINCA syndrome may provide more insights into the pathogenesis of cardiovascular disease.

Key words: ankle–brachial index, atherosclerosis, chronic infantile neurologic cutaneous and articular syndrome, cryopyrin-associated periodic syndromes, intima-media thickness, pulse wave velocity.

Introduction

It is well known that chronic inflammation is a predisposing factor for atherosclerosis. There has been considerable interest regarding the possible causal role of inflammation in the development of atherosclerosis in adult patients with RA, SLE and familial Mediterranean fever (FMF). Patients with SLE, APS or RA have increased mortality rates related to early atherosclerosis. Relative risk of 5 for myocardial infarction, 6–10 for stroke in SLE patients and 3.6 for cardiovascular deaths in RA patients has been reported [1]. Furthermore, the American Heart Association has reported that chronic inflammatory disease is one of the eight high-risk factors for atherosclerosis, even in children [2].

Cryopyrin-associated periodic syndromes (CAPS), including chronic infantile neurological cutaneous and articular (CINCA) syndrome, Muckle–Wells syndrome and familial cold autoinflammatory syndrome, are autosomal dominant autoinflammatory syndromes caused by heterozygous mutations of the *NLR family pyrin domain*

[1]Department of Pediatrics and [2]Department of Perinatal and Pediatric Medicine, Graduate School of Medical Sciences, Kyushu University, Fukuoka, Japan.

Submitted 25 November 2013; revised version accepted 11 March 2014.

Correspondence to: Kenichiro Yamamura, Department of Pediatrics, Graduate School of Medical Sciences, Kyushu University, 3-1-1, Maidashi, Higashi-ku, Fukuoka 812-8582 Japan.
E-mail: yamamura@pediatr.med.kyushu-u.ac.jp

containing 3 (*NLRP3*) gene. It has been reported that disease associated *NLRP3* mutation causes IL-1β oversecretion by caspase-1 activation. CINCA syndrome, the most severe form among them, is characterized by chronic systemic inflammation manifested as early onset of rash, fever, uveitis, chronic meningitis and joint symptoms [3]. However, there has been no previous report evaluating atherosclerosis in patients with CAPS.

Several physiological examinations are applied to assess atherosclerosis. Carotid intima–media thickness (cIMT) is known to be an indicator of atherosclerosis for adults and children [4]. In fact, increased cIMT has been shown in children with obesity, hyperlipidaemia and diabetes mellitus [5]. It has been reported that stiffness parameter β is more useful in detecting atherosclerotic changes in earlier stages than cIMT [6]. Also, pulse wave velocity (PWV) and ankle–brachial index (ABI) are simplified parameters of the severity of atherosclerosis and predictors of prognosis in adult patients with cardiovascular disease [7, 8]. The objective of this study is to assess the development and progression of atherosclerosis in young patients with CINCA syndrome by measuring cIMT, stiffness parameter β, PWV and ABI.

Patients and methods

Study population

Three patients (a 5-year-old boy [9], a 7-year-old girl [10] and a 15-year-old boy [11]) with CINCA syndrome and 19 age-matched healthy controls were enrolled in this study. *NLRP3* mutations were observed in all three patients. The parameters of atherosclerosis were investigated in these three patients who were in remission for 1 year after the initiation of canakinumab treatment. The Institutional Review Board of Kyushu University Hospital approved the study and informed consent was obtained from each subject.

Sonographic study

Carotid artery US was performed with an iE33 ultrasound machine (Philips, Amsterdam, The Netherlands) using an 11 MHz probe. Measurements were obtained with subjects in the supine position by experienced sonographers blinded to the subjects' clinical status. Ultrasonographic images of the right and left common carotid arteries (CCAs) of each subject at the lower third cervical region proximally and 1 cm above the carotid bulb distally in the longitudinal plane were obtained. CCA IMT measurements of the distal CCA posterior wall were done manually by the distance measurement system of the sonography device after magnification of the images. Three measurements were made in a non-neighbouring fashion within an ~1 cm segment from both the left and right CCA proximal and distal portions. The IMT was measured during end diastole. Mean IMT was calculated as the average of three consecutive measurements of maximum far wall thickness obtained from the CCA. Measurement of the internal diameter of the CCA was performed for three consecutive heartbeats. Intraobserver variability was 1.7% for IMT and 3.1% for arterial wall diameter measurements. The stiffness parameter β was calculated from this formula [12]: $\beta = [\ln(SBP/DBP)]/(\Delta D/D)$, where SBP is the systolic blood pressure, DBP is the diastolic blood pressure, D is carotid artery diastolic diameter and ΔD is the change in artery diameter during systole.

PWV and ABI

PWV and ABI were measured using a BP-203RPEIII (Omron Colin, Tokyo, Japan). PWV, ABI, the blood pressure of the extremities, ECG and heart sounds were synchronously measured and then automatically recorded. Electrodes were contacted on both wrists and a microphone was attached to the left margin of the sternum. The extremities were then wrapped by cuffs that were connected to a pulse monitor. The volume wave and time difference emitted from the pulse monitor were recorded. The pulse wave was defined as the value obtained by dividing the distance between the two points by the time spent in transferring the pulse. In the current study, the pulse wave was measured in the brachial artery and ankle (baPWV). The ABI was defined as the ratio between the systolic pressure measured in the ankle and that measured in the brachial artery.

Laboratory evaluation

In the morning, after an overnight fast, venous blood was sampled for the measurement of serum concentrations of glucose, total cholesterol, triglycerides and standard CRP.

Statistical analysis

Data are expressed as mean (S.D.). Differences between data were studied using the Student's *t* test. Analytical statistics of data between group comparisons of categorical data parameters were performed by using the chi-square test. Statistical significance was taken as $P < 0.05$. All statistical analyses were performed using JMP8 (SAS Institute, Tokyo, Japan).

Results

Clinical characteristics of the study group are presented in Table 1. Age, sex and triglyceride levels were similar between patients with CINCA syndrome and control subjects ($P = 0.65$, 0.53 and 0.17, respectively). Total cholesterol levels in CINCA syndrome patients were significantly lower than those in healthy controls, although they were within normal ranges in both groups. CRP concentrations in the patient group were significantly higher than in healthy controls [5.76 mm (S.D. 2.05) *vs* 0.08 (0.16), $P < 0.0001$].

All subjects tolerated the sonographic examination well. Sonographic study results and normal values of the parameters for the age of the patients [13, 14] are summarized in Table 2. Carotid artery analysis revealed that the IMT and stiffness parameter β of patients with CINCA syndrome were significantly higher than those of healthy controls [0.51 mm (S.D. 0.05) *vs* 0.44 (0.04), $P = 0.0021$, and 6.1 (S.D. 1.7) *vs* 3.9 (1.0), $P = 0.018$, respectively).

TABLE 1 Clinical and laboratory characteristics of the subjects

	Patient 1	Patient 2	Patient 3	CINCA syndrome ($n=3$), mean (S.D.)	Controls ($n=19$), mean (S.D.)	P-value
Gender, male/female	Male	Female	Male	2/1	9/10	0.53
Age, years	5	7	15	9.0 (5.3)	9.3 (4.3)	0.65
BMI, kg/m^2	16.0	15.5	16.8	16.1 (0.6)	17.3 (2.9)	0.51
Systolic blood pressure, mmHg	91	96	128	105 (20)	99 (8)	0.38
Diastolic blood pressure, mmHg	45	50	68	54 (12)	53 (4)	0.73
Total cholesterol, mg/dl	123	122	131	125 (5)	159 (17)	0.0046
Triglycerides, mg/dl	61	79	157	99 (51)	70 (28)	0.17
Glucose, mg/dl	93	85	102	94 (3)	94 (6)	0.95
CRP, mg/dl	0.26	1.62	5.55	2.48 (2.75)	0.08 (0.16)	<0.0001

CINCA syndrome: chronic infantile neurological cutaneous and articular syndrome.

TABLE 2 Ultrasonographic examination, baPWV and ABI in CINCA syndrome patients and control subjects

	Patient 1	Patient 2	Patient 3	CINCA syndrome ($n=3$), mean (S.D.)	Controls ($n=19$), mean (S.D.)	P-value
Intima–media thickness, mm (normal value for each age) [13]	0.47 (0.40)	0.5 (0.40)	0.57 (0.50)	0.51 (0.05)	0.44 (0.04)	0.0021
Systolic diameter, mm	5.5	5.8	5.8	5.7 (0.2)	6.2 (0.8)	0.30
Diastolic diameter, mm	4.8	5.2	5.4	5.1 (0.3)	5.3 (1.7)	0.63
Stiffness parameter β (normal value for each age) [14]	4.8 (3.4)	5.7 (3.7)	7.6 (4.5)	6.1 (1.7)	3.9 (1.0)	0.018
Right baPWV, cm/s	1068	920	1566	1185 (338)	850 (114)	0.0025
Left baPWV, cm/s	1053	1022	1587	1221 (318)	859 (114)	0.0014
Averaged baPWV, cm/s (normal value for each age) [15]	1061 (<941)	971 (<919)	1577 (1041)	1203 (328)	855 (114)	0.0017
Right ABI	1.15	0.91	0.98	1.00 (0.10)	1.04 (0.10)	0.67
Left ABI	1.16	0.95	0.92	0.99 (0.10)	1.06 (0.10)	0.48
Averaged ABI (normal value for each age) [15]	1.16 (>1.00)	0.93 (>1.00)	0.95 (>1.00)	0.99 (0.10)	1.05 (0.10)	0.54

CINCA syndrome: chronic infantile neurological cutaneous and articular syndrome; baPWV: brachial artery pulse wave velocity; ABI: ankle–brachial index.

The averaged baPWV of the patients was significantly higher than that of controls [1203 cm/s (S.D. 328) *vs* 855 (114), $P=0.017$) (Table 2). There was no significant difference in ABI between the two groups, although the values of two patients were lower than the normal range [15].

Discussion

In the present study we found that patients with CINCA syndrome develop atherosclerosis from early childhood. There have been many previous studies describing atherosclerosis associated with inflammatory diseases such as RA, SLE and FMF [1]. However, this is the first report showing the youngest group of patients who developed atherosclerosis associated with inflammatory disorders.

It has been shown that inflammation plays an important role in the development of atherosclerosis. The presence of macrophages and activated lymphocytes within the plaques supports the nature of an immune system-mediated inflammatory disorder of atherosclerosis. It has been shown that higher disease activity representing higher inflammatory burden is associated with increased cardiovascular events in patients with RA and SLE [16]. It may be induced by elevated inflammatory cytokines, which can cause the development of endothelial dysfunction in atherosclerotic processes. In addition, changes in lipid metabolism and a wide variety of immune and inflammatory alterations that directly affect the endothelium, vascular smooth muscle cells and inflammatory cellular components of the atherosclerotic plaque may also play important roles in the development and progression of atherosclerosis in patients. CINCA syndrome is the most severe form of CAPS, and patients display severe systemic inflammation from the neonatal period [3].

Therefore it is reasonable to assume that the progression of atherosclerosis from childhood in three patients with CINCA syndrome is closely related to chronic systemic inflammation. It was reported that the incidence of atherosclerosis could be reduced by aggressive disease-modifying therapies in patients with RA and SLE [16]. In patients with CINCA syndrome, we can investigate the association between inflammation and atherosclerosis without any effect of classical risk factors such as obesity, smoking, hyperlipidaemia or diabetes. This may provide a novel clue to clarify the role of inflammation in the development of atherosclerosis.

In patients with FMF and SLE, age and disease duration were reported to be associated with the severity of atherosclerosis [17]. In the present study we found that the oldest patient (patient 3) with the longest disease duration had the most advanced atherosclerosis, which is in line with this report. Early diagnosis and effective treatment for chronic inflammation in these patients have been emphasized in preventing cardiovascular disease because a negative correlation between the duration of anti-inflammatory treatment and IMT has been observed in SLE patients [18].

Interestingly, improvements in PWV and cIMT [19] were reported in patients with RA after sufficient infliximab treatment. In patients with CINCA syndrome, canakinumab was reported to induce rapid and sustained remission of symptoms [20]. It is possible that a significant improvement in atherosclerosis will be observed in our patients with CINCA syndrome after canakinumab treatment in the near future.

However, there are some limitations in the present study. First, our study contains only a small number of patients because of the extremely rare incidence of this disease. Second, the parameters investigated in this study are considerably variable with the age of the subjects. It is also possible that the values of the parameters change because of the measurement equipment. Multicentre and long-term follow-up analysis with standardized procedures and tools on a larger number of the patients are necessary to provide more precise information on the pathogenesis of atherosclerosis.

Conclusion

Patients with CINCA syndrome developed atherosclerosis from early childhood. Atherosclerosis in CINCA syndrome patients may be a prototype of cardiovascular disease predominantly induced by chronic inflammation.

Rheumatology key messages

- Patients with CINCA syndrome develop atherosclerosis from early childhood.
- This report shows the youngest group of patients who developed atherosclerosis associated with inflammatory disorders.
- Early treatment with anti-IL-1β antibody might be beneficial in preventing atherosclerosis in CINCA syndrome.

Acknowledgements

We thank Junji Kishimoto (Digital Medicine Initiative, Kyushu University Hospital, Fukuoka, Japan) for the contribution of statistical analysis.

Funding: This work was supported by a grant for Research on Intractable Diseases from the Ministry of Health, Labour and Welfare of Japan to T.H. and a grant-in-aid for scientific research from the Ministry of Education, Culture, Sports, Science, and Technology of Japan (24791072) to K.Y.

Disclosure statement: The authors have declared no conflicts of interest.

References

1 Tyrrell PN, Beyene J, Feldman BM *et al.* Rheumatic disease and carotid intima-media thickness: a systematic review and meta-analysis. Arterioscler Thromb Vasc Biol 2010;30:1014–26.

2 Kavey RE, Allada V, Daniels SR *et al.* Cardiovascular risk reduction in high-risk pediatric patients: a scientific statement from the American Heart Association Expert Panel on Population and Prevention Science; the Councils on Cardiovascular Disease in the Young, Epidemiology and Prevention, Nutrition, Physical Activity and Metabolism, High Blood Pressure Research, Cardiovascular Nursing, and the Kidney in Heart Disease; and the Interdisciplinary Working Group on Quality of Care and Outcomes Research: endorsed by the American Academy of Pediatrics. Circulation 2006;114:2710–38.

3 Kubota T, Koike R. Cryopyrin-associated periodic syndromes: background and therapeutics. Mod Rheumatol 2010;20:213–21.

4 Peters SA, den Ruijter HM, Bots ML, Moons KG. Improvements in risk stratification for the occurrence of cardiovascular disease by imaging subclinical atherosclerosis: a systematic review. Heart 2012;98:177–84.

5 Jarvisalo MJ, Putto-Laurila A, Jartti L *et al.* Carotid artery intima-media thickness in children with type 1 diabetes. Diabetes 2002;51:493–8.

6 Hirai T, Sasayama S, Kawasaki T, Yagi S. Stiffness of systemic arteries in patients with myocardial infarction. A noninvasive method to predict severity of coronary atherosclerosis. Circulation 1989;80:78–86.

7 Hirata K, Kawakami M, O'Rourke MF. Pulse wave analysis and pulse wave velocity: a review of blood pressure interpretation 100 years after Korotkov. Circ J 2006;70:1231–9.

8 Vlachopoulos C, Aznaouridis K, Terentes-Printzios D, Ioakeimidis N, Stefanadis C. Prediction of cardiovascular events and all-cause mortality with brachial-ankle elasticity index: a systematic review and meta-analysis. Hypertension 2012;60:556–62.

9 Takada H, Ishimura M, Inada H *et al.* Lipopolysaccharide-induced monocytic cell death for the diagnosis of mild neonatal-onset multisystem inflammatory disease. J Pediatr 2008;152:885–7.

10 Takada H, Kusuhara K, Nomura A *et al.* A novel CIAS1 mutation in a Japanese patient with chronic infantile neurological cutaneous and articular syndrome. Eur J Pediatr 2005;164:785–6.

11 Saito M, Nishikomori R, Kambe N *et al.* Disease-associated CIAS1 mutations induce monocyte death, revealing low-level mosaicism in mutation-negative cryopyrin-associated periodic syndrome patients. Blood 2008;111: 2132–41.

12 Mitsnefes MM, Kimball TR, Witt SA *et al.* Abnormal carotid artery structure and function in children and adolescents with successful renal transplantation. Circulation 2004; 110:97–101.

13 Jourdan C, Wuhl E, Litwin M *et al.* Normative values for intima-media thickness and distensibility of large arteries in healthy adolescents. J Hypertens 2005;23: 1707–15.

14 Sato A, Ichihashi K, Momoi M. Stiffness parameter B: changes with age in normal children. Neurosonology 2007;20:124–8.

15 Niboshi A, Hamaoka K, Sakata K, Inoue F. Characteristics of brachial-ankle pulse wave velocity in Japanese children. Eur J Pediatr 2006;165:625–9.

16 Roman MJ, Shanker BA, Davis A *et al.* Prevalence and correlates of accelerated atherosclerosis in systemic lupus erythematosus. N Engl J Med 2003;349: 2399–406.

17 Ugurlu S, Seyahi E, Cetinkaya F *et al.* Intima-media thickening in patients with familial Mediterranean fever. Rheumatology 2009;48:911–5.

18 Ristic GG, Lepic T, Glisic B *et al.* Rheumatoid arthritis is an independent risk factor for increased carotid intima-media thickness: impact of anti-inflammatory treatment. Rheumatology 2010;49:1076–81.

19 Del Porto F, Lagana B, Lai S *et al.* Response to anti-tumour necrosis factor alpha blockade is associated with reduction of carotid intima-media thickness in patients with active rheumatoid arthritis. Rheumatology 2007;46: 1111–5.

20 Kone-Paut I, Lachmann HJ, Kuemmerle-Deschner JB *et al.* Sustained remission of symptoms and improved health-related quality of life in patients with cryopyrin-associated periodic syndrome treated with canakinumab: results of a double-blind placebo-controlled randomized withdrawal study. Arthritis Res Ther 2011;13: R202.

Pediatr Transplantation 2014: 18: E208–E211

Pediatric Transplantation
DOI: 10.1111/petr.12297

Successful treatment of non-Hodgkin's lymphoma using R-CHOP in a patient with Wiskott–Aldrich syndrome followed by a reduced-intensity stem cell transplant

Koga Y, Takada H, Suminoe A, Ohga S, Hara T. (2014) Successful treatment of non-Hodgkin's lymphoma using R-CHOP in a patient with Wiskott–Aldrich syndrome followed by a reduced-intensity stem cell transplant. *Pediatr Transplant*, 18: E208–E211. DOI: 10.1111/petr.12297.

Abstract: WAS is an X-linked primary immunodeficiency characterized by microthrombocytopenia, eczema, recurrent infections, and increased incidence of autoimmunity and malignancy. HSCT is the only curative treatment for WAS. Herein, we report the case of a 17-yr-old boy with WAS who received an unrelated HSCT while in complete remission of diffuse large B-cell lymphoma after chemotherapy. Pretransplant conditioning consisted of fludarabine, busulfan, and total body irradiation (4 Gy). GvHD prophylaxis consisted of tacrolimus and short-course methotrexate. Following HSCT, rapid and stable engraftment was observed. Platelet count gradually increased, and the generalized eczema improved. The patient developed grade II acute GvHD and limited chronic GvHD on days 30 and 210, respectively, which resolved with immunosuppressive treatment. Symptoms caused by the reactivation of human herpes virus-6, BK virus, and VZV were observed from days 21, 60, and 96, respectively; they were resolved after conservative treatment and acyclovir administration. No other regimen-related toxicity was observed. Complete donor bone marrow chimerism was achieved one month after transplantation. RIST is an effective therapeutic option for older children with WAS accompanied by malignant lymphoma.

Yuhki Koga, Hidetoshi Takada, Aiko Suminoe, Shouichi Ohga and Toshiro Hara
Department of Pediatrics, Graduate school of Medical Sciences, Kyushu University, Fukuoka, Japan

Key words: Wiskott–Aldrich syndrome – malignant lymphoma – reduced-intensity stem cell transplantation – allogeneic bone marrow transplantation

Yuhki Koga, Department of Pediatrics, Graduate school of Medical Sciences, Kyushu University 3-1-1 Maidashi, Higashi-ku, Fukuoka 812-8582, Japan
Tel.: +81 92 642 5421
Fax: +81 92 642 5435
E-mail: yuuki-k@pediatr.med.kyushu-u.ac.jp

Accepted for publication 25 April 2014

WAS is a primary immunodeficiency disease characterized by microthrombocytopenia, eczema, and recurrent infection caused by mutations in the *WAS* gene. The WAS protein links cellular signals that activate Cdc42 to the active cytoskeleton (1, 2).

The estimated overall risk of developing malignancies in children with primary immunodeficiency is 4%; in WAS-affected children, this risk is approximately 100-fold greater than that expected in healthy children of similar age. Non-Hodgkin lymphoma, especially DLBCL, represents more than 60% of tumors occurring in children with immunodeficiency and is the most common malignancy observed in patients with WAS (3).

Patients with WAS require HSCT (4, 5). Factors, including the conditioning regimen, donor source, and the age and clinical status of the recipient, at the time of transplant affect the outcome of HSCT (6). RIST may be an option for reducing early transplantation-related morbidity and mortality in WAS patients with complications. On the other hand, incomplete reconstitution can lead to a risk of autoimmune disorder development (7).

Herein, we report a case of successful HSCT for a patient with WAS in complete remission of

Abbreviations: DLBCL, diffuse large B-cell lymphoma; EADR-G, early antigen-diffuse and restrict compex-IgG; EBNA, EBV nuclear antigen; EBV, Epstein–Barr virus; GvHD, graft-versus-host disease; HLA, human leukocyte antigen; HSCT, hematopoietic stem cell transplantation; RIST, reduced-intensity stem cell transplantation; VCA, viral capsid antigen; VZV, varicella–zoster virus; WAS, Wiskott–Aldrich syndrome.

DLBCL. RIST from unrelated HLA-matched donor led to complete donor chimerism.

Case report

A 17-yr-old boy presented to our hospital with persistent fever and axial lymphadenopathy. He had eczema, thrombocytopenia, and recurrent infections since early childhood. He was diagnosed as having WAS with a WAS protein gene mutation in exon 1 (41G deletion) and a defect in WAS protein, which was verified by Western blotting when he was five yr old. He did not have HLA-matched siblings. Parental consent for HSCT from an unrelated bone marrow donor was not obtained at that time. He had generalized eczema and scattered petechiae. Axillary lymph nodes were enlarged bilaterally, 5 cm in diameter.

Laboratory examination revealed normal white blood cell count (5.46×10^9/L) and thrombocytopenia (platelet count: 8×10^9/L). Serum concentrations of C-reactive protein and lactate dehydrogenase were 0.4 mg/dL (normal range: 0.0–0.1) and 389 IU/L (normal range: 119–229), respectively. Soluble interleukin-2 receptor concentration was within the normal range (383 IU/L, normal range: 206–713). Immunologic examination revealed NK activity of 12.1% lysis (normal range: 20.8–40.8%) and proliferative response against phytohemagglutinin with a stimulation index of 147 (normal range: 254–388). Serum antibody titers against EB virus were as follows: EB VCA IgG, VCA-IgM, VCA-IgA, EADR-G, EB early antigen IgG, and anti-EBNA titers were 320, <10, 10, 320, <10, and <10, respectively, indicating inappropriate antibody responses against the EB virus. PCR of EBV-DNA was below the detection limit ($<2 \times 10^2$ copy/mL).

Computed tomography of the chest and abdomen confirmed the axillary lymphadenopathy and revealed para-aortic and inguinal lymphadenopathy (Fig. 1a). Gallium scintigraphy revealed uptake into the same lesions (Fig. 1b). Biopsy specimens from the left axillary lymph nodes were compatible with DLBCL (Fig. 2).

Immunohistochemical staining revealed that the large lymphoid cells were positive for CD20, CD79a, and immunoglobulin κ chain. On the basis of these findings, the patient was diagnosed as DLBCL clinical stage III.

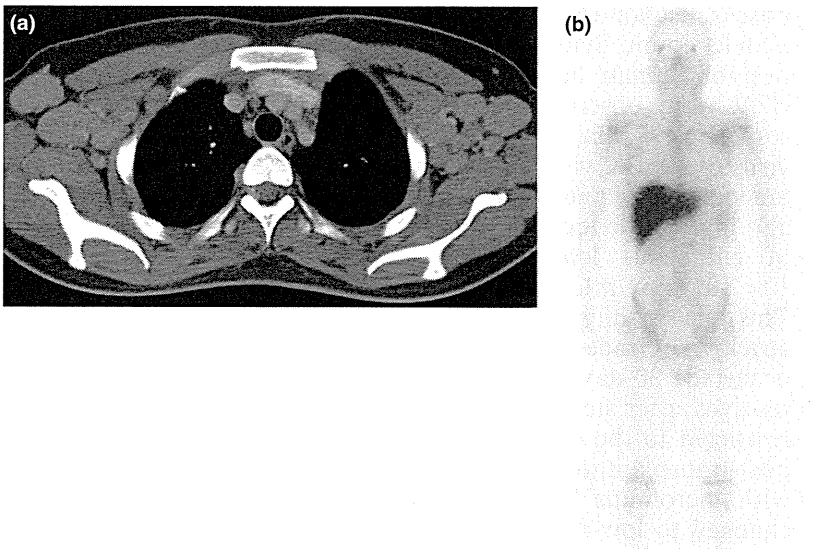

Fig. 1. Chest computed tomography and gallium scintigram. (a) Chest computed tomography. Arrows indicate bilateral axillary lymphadenopathy. (b) Gallium scintigram. Significant uptake into the axillary, para-aortic, and inguinal lymph nodes on both sides is observed.

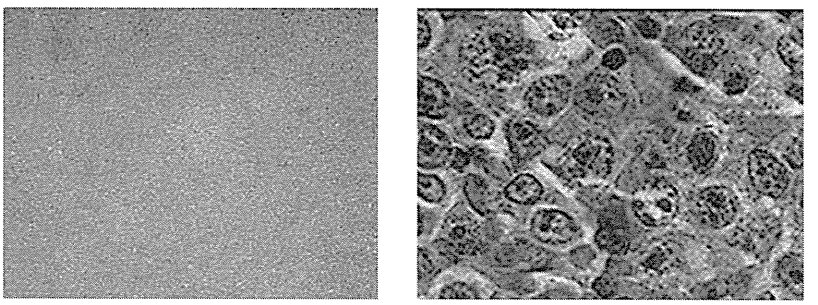

Fig. 2. Biopsy findings from the left axillary lymph nodes. The absence of follicular structures and diffusely proliferative medium-to-large lymphoid cells with Russell bodies and plasmacytic differentiation are observed (hematoxylin–eosin stain, left: ×100, right: ×400).

He achieved complete remission after treatment with chemotherapy consisting of six cycles of R-CHOP (i.e., rituximab, cyclophosphamide, doxorubicin, vincristine, and prednisone). He subsequently underwent HSCT from an HLA-matched unrelated bone marrow donor after receiving a conditioning regimen comprising fludarabine (30 mg/m^2 on days −9 to −4), busulfan (0.8 mg/kg i.v. q six h on days −5 and −4), and total body irradiation (2 Gy, twice/day on day −3); the area under the curve of busulfan was not measured. GvHD prophylaxis consisted of tacrolimus (0.3 mg/kg/day continuous i.v. from day −1) and short-course methotrexate (15 mg/m^2 on day 1 and 10 mg/m^2 on days 3 and 6). The number of infused nucleated cells was 1.8×10^8/kg (CD34 cell count was not performed). Neutrophil (>0.5×10^9/L) and platelet engraftment (>20×10^9/L) were achieved on days 19 and 26, respectively. Post-transplantation immune reconstitution up to the ninth month showed CD3, CD19, and CD56 counts were 480, 12, and 525 cells/μL on day 30 and 320, 159, and 557 cells/μL on day 90, respectively. Engraftment studies using short tandem repeat analysis of the bone marrow revealed 100% donor chimerism one month and one yr post-HSCT. At five yr post-transplantation, the patient has normal platelet count. Symptoms caused by the reactivation of human herpes virus-6, BK virus, and VZV were observed on days 21, 60, and 96, respectively. The symptoms of human herpes virus-6 and BK virus reactivation resolved spontaneously. The patient developed abdominal pain and high-grade fever on day 96. Despite the lack of cutaneous lesions, a VZV PCR showed 1×10^3 copy/mL, indicating VZV reactivation. This successfully resolved after treatment with acyclovir. Grade II acute GvHD (gut, stage 1) occurred 30 days post-transplantation, which resolved after steroid treatment. Chronic GvHD restricted to the oral mucosa occurred 210 days post-transplantation and was successfully treated with tacrolimus for one yr; however, this was changed to low-dose weekly methotrexate treatment, because the patient's condition gradually worsened. Because methotrexate was effective, it was continued for two yr. The patient is alive as of five yr post-transplantation without any symptoms of WAS, post-transplantation complications, or autoimmune diseases.

Discussion

The overall outcome of patients with WAS without stem cell transplantation remains poor (8, 9). The best transplantation outcome is achieved with myeloablative conditioning and HLA-identical sibling donors or HLA-matched unrelated donors when the recipient is younger than five yr at the time of transplantation (4, 10). Although the outcome of HSCT from an HLA-mismatched related donor remains extremely poor (11), the other factors influencing HSCT outcome in older children with WAS remain largely unknown. In addition, optimal conditioning for HSCT in WAS patients with complications such as malignant disorders is an important issue that must be addressed in the future studies.

Many children with primary immunodeficiency disease may have comorbidities at the time of HSCT. Therefore, conventional myeloablative preparation may be associated with significant treatment-related toxicity as well as long-term sequelae (12). Over the past decade, RIST has become a well-established approach in adult patients with malignant disease, extending curative HSCT to older individuals and patients with comorbidities otherwise ineligible for myeloablative procedures. HSCT is reported to be effective for children with WAS even after the development of lymphoma (13). RIST can be an important option for the treatment of older children with WAS, who are likely to have active infections and organ damage due to complications. Longhurst et al. (14) report the case of a 26-yr-old man with WAS who had undergone RIST because of severe infections and vasculitis, although engraftment and immunorestoration were only partial.

Chronic GvHD-independent autoimmunity has been observed in patients with WAS after HSCT and is strongly associated with a mixed/split chimerism status (7, 15). On the other hand, Shin et al. (16) report that the incidence of post-HSCT autoimmune cytopenia is high, even in patients with WAS who have received myeloablative HSCT, and that it is not associated with post-transplantation mixed chimerism. A small population of residual host B cells and plasma cells that failed to be detected by chimerism analysis may play a key role in the pathogenesis of WAS. Because of the patient's underlying diagnosis of WAS and DLBCL, we decided to perform a RIST to decrease the risk of death post-transplant. Full-donor chimerism was achieved, and the patient did not have any signs of autoimmune disorders or fatal infectious disease after HSCT. Therefore, the reduced-intensity regimen was sufficient for conditioning after chemotherapy for DLBCL.

The outcomes of patients receiving transplantation from mismatched family donors and HSCT from an unrelated donor have improved

recently (16, 17). This could be attributed to the selection of unrelated donors by high-resolution HLA-typing, improved viral monitoring, and the use of effective immunosuppressive drugs.

In conclusion, RIST from unrelated HLA-matched donor led to complete donor chimerism in a patient with WAS in complete remission of DLBCL. Therefore, RIST is an effective therapeutic option for older children with WAS accompanied by malignant lymphoma. Nevertheless, further evaluation and follow-up studies are required to clarify the safety and effectiveness of RIST for patients with WAS, especially in older children with malignant complications.

References

1. Miki H, Miura K, Takenawa T. N-WASP, a novel actin-polymerizing protein, regulates the cortical cytoskeletal rearrangement in a PIP-2 dependent manner downstream of tyrosine kinases. EMBO J 1996: 15: 5326–5335.
2. Miki H, Suetsugu S, Takenawa T. WAVE, a novel WASP-family protein involved in actin reorganization induced by Rac. EMBO J 1998: 17: 6932–6941.
3. Coccia P, Mastrangelo S, Ruggiero A, et al. Treatment of pharyngeal non-Hodgkin lymphoma in a patient with Wiskott-Aldrich syndrome. Pediatr Blood Cancer 2012: 59: 318–319.
4. Filipovich AH, Stone JV, Tomany SC, et al. Impact of donor type on outcome of bone marrow transplantation for Wiskott-Aldrich syndrome: Collaborative study of the International Bone Marrow Transplant Registry and the National Marrow Donor Program. Blood 2001: 97: 1598–1603.
5. Nortarangelo LD, Miao CH, Ochs HD. Wiskott-Aldrich syndrome. Curr Opin Hematol 2008: 15: 30–36.
6. Pai SY, Nortarangelo LD. Hematopoietic cell transplantation for Wiskott-Aldrich syndrome: Advances in biology and future directions for treatment. Immunol Allergy Clin North Am 2010: 30: 179–194.
7. Ozsahin H, Cavazzana-Calvo M, Nortarangelo LD, et al. Long-term outcome following hematopoietic stem-cell transplantation in Wiskott-Aldrich syndrome: Collaborative study of the European Society for Immunodeficiencies and European Group for Blood and Marrow Transplantation. Blood 2008: 111: 439–445.
8. Lum LG, Tubergen DG, Corash L, Blaese RM. Splenectomy in the management of thrombocytopenia of the Wiskott-Aldrich syndrome. N Engl J Med 1980: 302: 892–896.
9. Massaad MJ, Ramesh N, Geha RS. Wiskott-Aldrich syndrome: A comprehensive review. Ann NY Acad Sci 2013: 1285: 26–43.
10. Kobayashi R, Ariga T, Nonoyama S, et al. Outcome in patients with Wiskott-Aldrich syndrome following stem cell transplantation: An analysis of 57 patients in Japan. Br J Haematol 2006: 135: 362–366.
11. Mahlaoui N, Pellier I, Mignot C, et al. Characteristics and outcome of early-onset, severe forms of Wiskott-Aldrich syndrome. Blood 2013: 121: 1510–1516.
12. Veys P. Reduced intensity transplantation for primary immunodeficiency disorders. Pediatr Rep 2011: 3(Suppl 2): e11.
13. Tavil B, Erdem AY, Azik F, et al. Successful allogeneic hemopoietic stem cell transplantation in a case of Wiskott-Aldrich syndrome and non-Hodgkin lymphoma. Pediatr Transplant 2013: 17: E146–E148.
14. Longhurst HJ, Taussig D, Haque T, et al. Non-myeloablative bone marrow transplantation in an adult with Wiskott-Aldrich syndrome. Br J Haematol 2002: 116: 497–499.
15. Ochs HD, Filipovich AH, Veys P, Cowan MJ, Kapoor N. Wiskott-Aldrich syndrome: Diagnosis, clinical and laboratory manifestations, and treatment. Biol Blood Marrow Transplant 2009: 15: 84–90.
16. Shin CR, Kim MO, Li D, et al. Outcomes following hematopoietic cell transplantation for Wiskott-Aldrich syndrome. Bone Marrow Transplant 2012: 47: 1428–1435.
17. Moratto D, Giliani S, Bonfim C, et al. Long-term outcome and lineage-specific chimerism in 194 patients with Wiskott-Aldrich syndrome treated by hematopoietic cell transplantation in the period 1980-2009: An international collaborative study. Blood 2011: 118: 1675–1684.

The Journal of Immunology

Activation of an Innate Immune Receptor, Nod1, Accelerates Atherogenesis in *Apoe*$^{-/-}$ Mice

Shunsuke Kanno, Hisanori Nishio, Tamami Tanaka, Yoshitomo Motomura, Kenji Murata, Kenji Ihara, Mitsuho Onimaru, Sho Yamasaki, Hajime Kono, Katsuo Sueishi and Toshiro Hara

J Immunol 2015; 194:773-780; Prepublished online 8 December 2014;
doi: 10.4049/jimmunol.1302841
http://www.jimmunol.org/content/194/2/773

The Journal of Immunology is published twice each month by The American Association of Immunologists, Inc., 9650 Rockville Pike, Bethesda, MD 20814-3994.

Print ISSN: 0022-1767 Online ISSN: 1550-6606.

Activation of an Innate Immune Receptor, Nod1, Accelerates Atherogenesis in *Apoe*$^{-/-}$ Mice

Shunsuke Kanno,* Hisanori Nishio,*,† Tamami Tanaka,* Yoshitomo Motomura,‡ Kenji Murata,* Kenji Ihara,* Mitsuho Onimaru,§ Sho Yamasaki,‡ Hajime Kono,¶ Katsuo Sueishi,‖ and Toshiro Hara*

Atherosclerosis is essentially a vascular inflammatory process in the presence of an excess amount of lipid. We have recently reported that oral administration of a nucleotide-binding oligomerization domain (Nod)-1 ligand, FK565, induced vascular inflammation in vivo. No studies, however, have proven the association between Nod1 and atherosclerosis in vivo. To investigate a potential role of NOD1 in atherogenesis, we orally administered FK565 to apolipoprotein E knockout (*Apoe*$^{-/-}$) mice for 4 wk intermittently and performed quantification of atherosclerotic lesions in aortic roots and aortas, immunohistochemical analyses, and microarray-based gene expression profiling of aortic roots. FK565 administration accelerated the development of atherosclerosis in *Apoe*$^{-/-}$ mice, and the effect was dependent on Nod1 in non–bone marrow origin cells by bone marrow transplantation experiments. Immunohistochemical studies revealed the increases in the accumulation of macrophages and CD3 T cells within the plaques in aortic roots. Gene expression analyses of aortic roots demonstrated a marked upregulation of the *Ccl5* gene during early stage of atherogenesis, and the treatment with Ccl5 antagonist significantly inhibited the acceleration of atherosclerosis in FK565-administered *Apoe*$^{-/-}$ mice. Additionally, as compared with *Apoe*$^{-/-}$ mice, *Apoe* and *Nod1* double-knockout mice showed reduced development of atherosclerotic lesions from the early stage as well as their delayed progression and a significant reduction in *Ccl5* mRNA levels at 9 wk of age. Data in the present study show that the Nod1 signaling pathway in non–bone marrow-derived cells contributes to the development of atherosclerosis. *The Journal of Immunology*, **2015, 194: 773–780.**

Atherosclerosis is a chronic inflammatory disease of vessel walls, characterized by the accumulation of leukocytes and their subsequent differentiation into cholesterol-laden foam cells (1). Innate and acquired immune systems are considered to be associated with the development of atherosclerosis (2–4). Concerning the innate immunity, epidemiological studies and animal experiments showed that infectious agents and their components contribute to the local chronic inflammatory process underlying atherosclerosis (4–7). The innate immune receptors recognize structurally conserved moieties and work as pattern recognition receptors (PRRs) such as TLRs, nucleotide oligomerization domain–like receptors (NLRs), retinoic acid–inducible gene-I-like receptors or C-type lectin receptors (8). Among PRR families, there is a line of evidence that TLRs, especially TLR4, TLR2, and their signaling molecule, MyD88 (7, 9, 10), play important roles in the development of atherosclerosis by initiating an inflammatory response to several pathogenic bacteria such as *Chlamydophila pneumoniae* or *Porphyromonas gingivalis* (5, 6).

With respect to NLRs, only a limited number of studies have shown that NLRs might be involved in atherosclerosis (11, 12). More than 20 NLRs have been identified in humans (8). Nucleotide-binding oligomerization domain (NOD)-1 is an intracellular sensor of bacterial peptidoglycan (PGN), and it is constitutively expressed in many types of cells, including endothelial cells (13, 14). NOD1 specifically recognizes a diaminopimelic acid–containing dipeptide, derived mostly from bacteria (13), and activates the signal pathway via the transcription factor NF-κB (14, 15). Recently, pure synthetic ligands for NLRs, such as FK156 and FK565 for NOD1 or MDP for NOD2, have been available for studies on the biological significance of these receptors. We have recently reported that oral administration of a synthetic Nod1 ligand FK565 efficiently induced acute vasculitis in mice (16). Therefore, it would make sense to investigate the contribution of a long-term exposure of a small dose of NOD1 ligand to the development of atherosclerosis, a chronic vascular inflammatory disease.

In this study, we show that oral administration of FK565 accelerated the development of atherosclerosis in apolipoprotein E knockout (*Apoe*$^{-/-}$) mice, and the effect was dependent on Nod1 in non–bone marrow-derived cells by transplantation experiments. By microarray analysis, we found that *Ccl5* expression was sig-

*Department of Pediatrics, Graduate School of Medical Sciences, Kyushu University, Fukuoka 812-8582, Japan; †Center for the Study of Global Infection, Kyushu University Hospital, Fukuoka 812-8582, Japan; ‡Division of Molecular Immunology, Medical Institute of Bioregulation, Kyushu University 812-8582, Fukuoka, Japan; §Division of Pathophysiological and Experimental Pathology, Department of Pathology, Kyushu University, Fukuoka 812-8582, Japan; ¶Department of Internal Medicine, Teikyo University School of Medicine, Tokyo 173-8605, Japan; and ‖Department of Research and Education, National Hospital Organization Fukuoka–Higashi Medical Center, Fukuoka 811-3195, Japan

Received for publication October 21, 2013. Accepted for publication November 13, 2014.

This work was supported by grants from the Japan Society for the Promotion of Science and Health and Labour Sciences Research Grants from the Ministry of Health, Labor and Welfare, Japan.

The microarray data presented in this article have been submitted to the Gene Expression Omnibus (http://www.ncbi.nlm.nih.gov/geo/) under accession number GSE48947.

Address correspondence and reprint requests to Dr. Shunsuke Kanno, Department of Pediatrics, Graduate School of Medical Sciences, Kyushu University, 3-1-1 Maidashi, Higashi-ku, Fukuoka, 812-8582, Japan. E-mail address: kannos@pediatr.med.kyushu-u.ac.jp

The online version of this article contains supplemental material.

Abbreviations used in this article: Apoe, apolipoprotein E; EVG, Elastica–van Gieson; NLR, nucleotide oligomerization domain–like receptor; NOD, nucleotide-binding oligomerization domain; PGN, peptidoglycan; PRR, pattern recognition receptor; RIP2, receptor-interacting protein 2; α-SMA, α–smooth muscle actin.

www.jimmunol.org/cgi/doi/10.4049/jimmunol.1302841

nificantly upregulated by FK565 administration in aortic roots during early stage of atherogenesis, and the treatment with Ccl5 antagonist significantly inhibited the acceleration of atherosclerosis in FK565-administered *Apoe*$^{-/-}$ mice. Finally, we demonstrated that Nod1 deficiency resulted in reduced development of atherosclerotic lesions as well as their delayed progression in *Apoe*$^{-/-}$ mice, indicating the contribution of Nod1 ligand to the development of atherosclerosis.

Materials and Methods

Animals and bone marrow transplantation

C57BL/6J *Apoe*$^{-/-}$ mice were purchased from The Jackson Laboratory. *Nod1*$^{-/-}$ mice in the C57BL/6 background were a gift from Tak Mak, University Health Network. *Nod1*$^{-/-}$ mice were crossed with *Apoe*$^{-/-}$ C57BL/6 mice. Heterozygous mice were intercrossed to generate homozygous *Apoe*$^{-/-}$ mice bearing combinations of *Nod1*$^{+/+}$ and *Nod1*$^{-/-}$ mice. The genotype for *Apoe* or *Nod1* was confirmed using primers and conditions described in the The Jackson Laboratory Web site or the previous report (17), respectively. All mice were fed a normal chow diet and housed in a specific pathogen-free environment throughout the experiment. Drinking water and food for mice did not contain Nod1-stimulatory activity by a bioassay using HEK-Blue murine NOD1 cells (InvivoGen, San Diego, CA), which were HEK293 cells carrying a NF-κB reporter and transfected with a Nod1 construct. The study protocol was reviewed and approved by the Animal Care and Treatment Committee of Kyushu University.

For bone marrow transplantation studies, 9-wk-old male *Apoe*$^{-/-}$*Nod1*$^{-/-}$ mice and *Apoe*$^{-/-}$*Nod1*$^{+/+}$ mice received 8 Gy total body irradiation to eliminate endogenous bone marrow stem cells and most of the bone marrow–derived cells, including macrophages. Bone marrow cells for transplantation into the irradiated mice were prepared by flushing both femurs of male *Apoe*$^{-/-}$*Nod1*$^{-/-}$ or *Apoe*$^{-/-}$*Nod1*$^{+/+}$ mice. Donor cells were washed, suspended in sterile RPMI 1640 medium with 2% FCS, and concentrated to 1×10^8 cells/ml. Three hours after irradiation, 1×10^7 bone marrow cells were injected into the tail vein of a mouse. Successful reconstitution was confirmed by PCR genotyping of recipient mouse peripheral blood cells.

FK565 administration and Met-RANTES treatment

FK565, a synthetic and pure Nod1 ligand, was supplied by Astellas Pharma (Tokyo, Japan). At 5 wk of age, mice were randomized to FK565-administered and nonadministered groups. The administration protocol was as follows: two doses of FK565 solution (10 or 50 μg), reconstituted at 10 μg/μl in sterile distilled H_2O, was orally administered once a day for 2 consecutive days and then observed for the following 5 d per week. This course of the intermittent administration was continued for 4 wk, and mice were euthanized 6 d after the last administration. For the transplanted mice, FK565 was administered for four courses from 7 wk after bone marrow transplantation and euthanized at 20 wk of age. After euthanasia, serum was obtained from the vena cava after an overnight fast.

Because the Ccl5 antagonist Met-RANTES has been used in vivo in animal models of atherosclerosis, we determined the protocol of Met-RANTES treatment according to previous reports (18–20) with minor modifications. Met-RANTES (R&D Systems, Minneapolis, MN) was administered i.p. in a single dose of 50 μg diluted in PBS 30 min before FK565 administration. In parallel, control mice received a similar volume of sterile PBS.

Antibiotic treatment protocol

Mice were treated with 1 g/l ampicillin (Wako Pure Chemicals, Osaka, Japan) dissolved in drinking water, as well as an antibiotic concoction consisting of 5 mg/ml vancomycin, 10 mg/ml neomycin, and 10 mg/ml metronidazole (all from Wako Pure Chemicals) by oral gavage every 24 h according to the method as described (21). Gavage volume of 20 ml/kg body weight was delivered with a polytetrafluoroethylene tube with prior sedation of the mice. The antibiotic administration was initiated at 5 wk of age and continued for 5 wk from 1 wk before 4 wk FK565 administration.

Intestinal depletion was assessed by collecting feces, homogenizing in 1 ml sterile PBS, and serially diluting and plating on trypticase soy agar with 5% sheep blood (BD Biosciences, Franklin Lakes, NJ) for 48 h at 37°C aerobically or in an anaerobic chamber (AnaeroPack system; Mitsubishi Gas Chemical, Tokyo, Japan). The number of bacteria per milligram of feces was calculated based on the CFU counted in each serial dilution.

Histological and immunohistological analyses of aortic roots

After mice were euthanized, the hearts were removed rapidly after perfusion with PBS. The hearts were embedded in optimal cutting temperature compound (Sakura Finetek Japan, Tokyo, Japan) and quickly frozen in liquid nitrogen or 4% paraformaldehyde-fixed and paraffin-embedded for histological and immunohistological analyses. Sixty serial cross-sections (6 μm thick) of the aortic root were prepared from the site where the three aortic valves first appeared according to the method as described (22). The atherosclerotic lesions in the aortic root were investigated at six locations, each separated by 60 μm. Three serial frozen sections prepared from each location were conventionally stained with Sudan IV (Tokyo Kasei Kogyo, Tokyo, Japan), Elastica–van Gieson (EVG), and H&E stains. Similarly, seven serial paraffin-embedded sections prepared from each location were stained with H&E, EVG, MOMA-2 (macrophage)–specific Ab (1:100; AbD Serotec, Raleigh, NC), CD3 (T cell)–specific Ab (1:500; Abcam, Cambridge, U.K.), NIMP-R14 (neutrophil)–specific Ab (1:500; Abcam), α–smooth muscle actin (α-SMA)–specific Ab (1:100; Dako, Glostrup, Denmark), and Ccl5-specific Ab (1:10; R&D Systems). As a negative control, nonimmune IgG or isotype control was used. Detection and visualization of primary Ab binding was done as described (16). For quantitative estimation of the plaque contents, we analyzed absolute areas or numbers of cells staining positive for a respective marker within the plaque area by using Adobe Photoshop CS5 and National Institutes of Health ImageJ software. The average value for the six locations for each animal was used for analysis.

Assessment of atherosclerosis in aortas

Immediately after mice were euthanized, the aorta was dissected from the proximal ascending aorta to the bifurcation of the iliac artery. The adventitial tissue was carefully removed, and then the aorta was opened longitudinally, fixed in 10% buffered formalin overnight, stained with Sudan IV, pinned on a black wax surface, and photographed for quantification of en face plaque areas. En face images were obtained by a stereomicroscope (SteREO Lumar V12; Carl Zeiss, Oberkochen, Germany) equipped with a digital camera (AxioCam MRc5; Carl Zeiss) and analyzed by Adobe Photoshop CS5 and National Institutes of Health ImageJ software. Lipid lesion formation was analyzed by the determination of the percentage area stained with Sudan IV to the total aortic area. Quantification of atherosclerotic lesions was performed by a single observer blinded to the experimental protocol.

Microarray analysis

To obtain sufficient amount of RNA for microarray analysis, the aortic roots removed from three animals were mixed, homogenized, and used as one sample. Two independent experiments were performed. Total RNA was extracted with an RNeasy fibrous tissue kit (Qiagen, Hilden, Germany) and amplified using an amino allyl MessageAmp II aRNA amplification kit (Ambion, Austin, TX). Double-stranded cDNA was synthesized from total RNA using oligo(dT) primer with a T7 RNA polymerase promoter site added to the 3′ end. Then, in vitro transcription was performed in the presence of amino allyl uridine-5′-triphosphate to produce multiple copies of amino allyl-labeled cRNA. Amino allyl–labeled cRNA was purified, reacted with *N*-hydroxy succinimide esters of Cy3 (GE Healthcare, Little Chalfont, U.K.) using NimbleGen's protocol and hybridized for 19 h at 42°C to the Mouse Gene Expression 12 × 135K array (100718_MM9_EXP_HX12; Roche NimbleGen, Madison, WI) consisting of 44,170 genes. The arrays were scanned on GenePix 4000B (Molecular Devices, Sunnyvale, CA). The averages of triplicate spot intensities were extracted using NimbleScan v2.5 (Roche NimbleGen) and processed using robust multiarray analysis method (16). The scaled gene expression values were imported into GeneSpring 11.5.1 software (Agilent Technologies, Santa Clara, CA) for preprocessing and data analysis (16). The expression value of each gene was normalized to the 75th percentile shift expression of all genes. Probe sets were deleted from subsequent analysis when they were displayed an absolute value <30 in all experiments. The fold change was calculated as the ratio of the two group means based on the observed signal values. Microarray data were deposited in Gene Expression Omnibus (http://www.ncbi.nlm.nih.gov/geo/) under accession no. GSE48947.

Quantitative real-time RT-PCR

Total RNA was extracted from the aortic root using RNeasy fibrous tissue, followed by cDNA synthesis using a high-capacity RNA-to-cDNA kit (Applied Biosystems, Foster City, CA). Mouse *Ccl5*, *Cxcl16*, *Ccl8*, and *Gapdh* expression levels were analyzed by TaqMan gene expression assays Mm01302427_m1, Mm00469712_m1, Mm01297183_m1, and Mn-99999915_g1 (Applied Biosystems), consisting of a 20× mix of unlabeled PCR primers and a TaqMan MGB probe (FAM dye-labeled), and TaqMan gene expression master mix (Applied Biosystems). Mouse *Gapdh* was used as internal controls. These TaqMan probes were labeled with the quencher TAMRA (emission I, 582 nm) at the 3′ end through a linker-arm nucleotide. The mRNA expression levels of the targeted genes were quantified by the StepOne real-time PCR system and the StepOne software

v2.1 (Applied Biosystems). To calculate the relative expression level, the level of gene expression was divided by that of *Gapdh*. All experiments were carried out in duplicate and repeated three times for confirmation.

Serum lipid, glucose, and insulin analyses

Total cholesterol and triglyceride concentrations in the murine sera were measured with a LabAssay cholesterol kit and a LabAssay triglyceride kit (Wako Pure Chemicals), respectively. Blood glucose levels were determined with a Medisafe-Mini glucose meter (Terumo, Tokyo, Japan). Serum insulin levels were measured with a mouse insulin ELISA kit (Mercodia, Uppsala, Sweden). The homeostasis model assessment of insulin resistance index ([glucose (mg/dl) × insulin (μU/ml)]/405) was calculated.

Statistical analysis

Data were analyzed by Student *t* test, Dunnett test, or Tukey–Kramer honestly significant difference test using JMP version 8.0 (SAS Institute, Cary, NC). Values of $p < 0.05$ were considered statistically significant.

Results

Activation of Nod1 by the orally administered agonist accelerates atherogenesis in Apoe$^{-/-}$ *mice*

To investigate the effect of a Nod1 ligand on atherosclerosis, we orally administered FK565, a pure synthetic Nod1 ligand, to *Apoe*$^{-/-}$ male mice fed a chow diet. After preliminary experiments with orally administered FK565 at different doses consecutively or intermittently in *Apoe*$^{-/-}$ mice (data not shown), we analyzed the effect of orally administered FK565 on 9-wk-old *Apoe*$^{-/-}$ mice at 10 or 50 μg twice a week for 4 wk from 5 wk of age (Fig. 1A). No significant differences between the body weight and serum cholesterol and triglyceride levels of both groups of mice were observed (Supplemental Table I). Compared with the nonadministered group, a dose-dependent effect of FK565 was observed in the development of atherosclerosis in aortic roots with the lesion volumes of 1.85-fold (85%) increase at 10 μg and 5.49-fold (449%) increase at 50 μg FK565 in the FK565-administered group (Fig. 1B, 1D). In the FK565-administered group, a similar effect was also observed on the plaque formation in aortas of 1.10-fold (10%) increase at 10 μg and 33.9-fold (3289%) increase at 50 μg FK565 (Fig. 1C, 1E). To confirm the specificity of the FK565 treatment for Nod1, we studied *Apoe*$^{-/-}$ *Nod1*$^{-/-}$ mice in the same manner. There were no differences in the body weight and serum cholesterol or triglyceride levels in both groups of mice (Supplemental Table I). The plaque formation results showed no significant differences between FK565-administered *Apoe*$^{-/-}$*Nod1*$^{-/-}$ mice and nonadministered mice (Fig. 1D, 1E). These results clearly demonstrated that oral administration of a pure synthetic Nod1 ligand accelerated the development of atherosclerosis in *Apoe*$^{-/-}$ mice in a Nod1-dependent manner.

To rule out the possibility that oral administration of FK565 alters the composition of gut commensal bacteria and the dysbiosis induces acceleration of atherosclerosis, we depleted the intestinal microbiota by providing antibiotics in drinking water and with oral gavage of the antibiotic concoction according to the previous report (21). Even in gut flora–depleted mice, FK565 administration accelerated the development of atherosclerosis, suggesting that the acceleration of atherosclerosis by orally administered FK565 does not depend on alteration of the composition of gut commensal bacteria (Supplemental Fig. 1).

Immunohistochemical studies of atherosclerotic lesions by a Nod1 ligand

To explore the effects of Nod1 ligand on the formation of atherosclerotic lesions, we performed immunohistochemical studies of vessel-wall constituents within the plaques in aortic roots. FK565-administered *Apoe*$^{-/-}$ mice showed a significantly higher level of macrophage and T cell infiltration within the plaques than did nonadministered *Apoe*$^{-/-}$ mice. Neutrophil numbers within the plaques in FK565-administered *Apoe*$^{-/-}$ mice also showed an

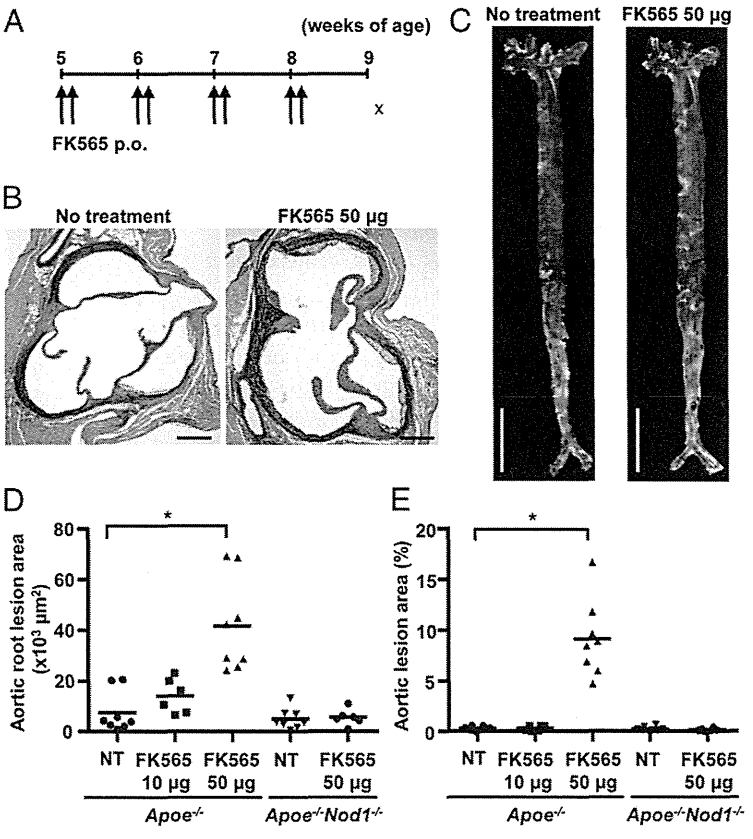

FIGURE 1. Acceleration of atherosclerosis by oral administration of FK565 in *Apoe*$^{-/-}$ mice. (**A**) Protocol for intermittent administration of FK565 (10 or 50 μg once a day, 2 d/wk, 4 wk) as described in *Materials and Methods*. p.o., per os. (**B** and **C**) Representative aortic roots (B) stained with EVG and aortas (C) stained with Sudan IV in *Apoe*$^{-/-}$ mice with or without FK565 administration at 9 wk of age. Scale bars, 200 μm (B) and 500 μm (C). (**D** and **E**) Quantification of atherosclerotic lesion areas of aortic roots (D) and aortas (E) in *Apoe*$^{-/-}$ mice with or without FK565 administration at 9 wk of age. Bars represent means (n = 6–8/group). *$p < 0.01$ versus nonadministered mice with each genotype (Dunnett test). NT, no treatment.

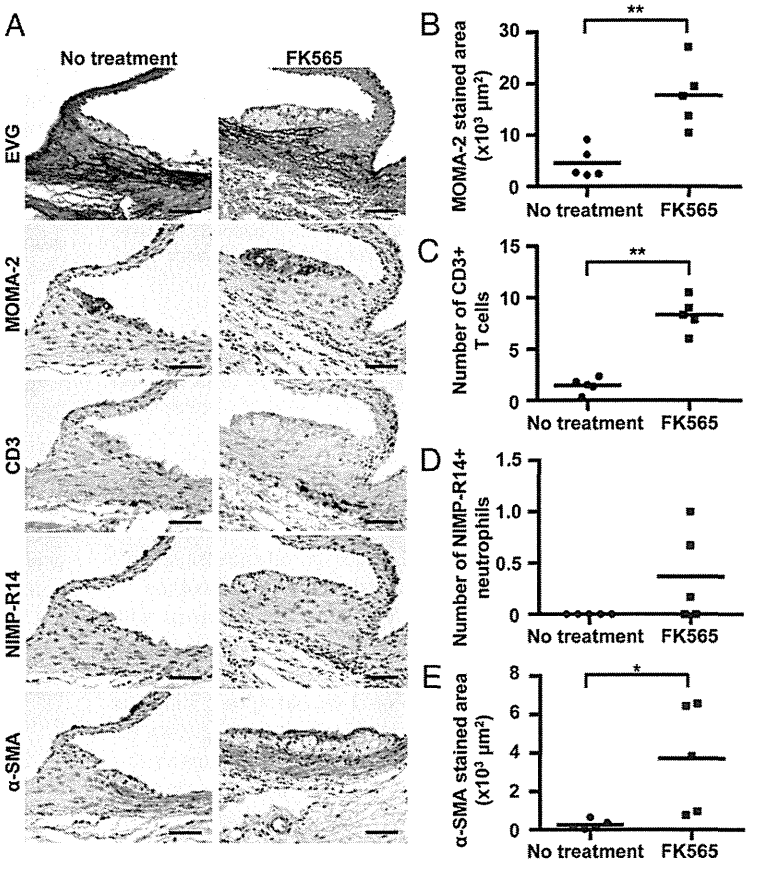

FIGURE 2. Immunohistochemical studies of atherosclerotic lesions by oral administration of FK565. (**A**) Representative aortic roots stained with EVG, MOMA-2, CD3, NIMP-R14, and α-SMA in *Apoe*$^{-/-}$ mice with or without FK565 administration at 9 wk of age. Scale bars, 50 μm. (**B–E**) Quantification of areas or numbers of cells positively stained for MOMA-2, CD3, NIMP-R14, and α-SMA within plaques in *Apoe*$^{-/-}$ mice with or without FK565 administration at 9 wk of age. Bars represent means (n = 5/group). *$p < 0.05$, **$p < 0.01$ (Student t test).

increasing tendency than did those in nonadministered *Apoe*$^{-/-}$ mice, although statistically not significant (Fig. 2A–D).

The previous report demonstrated that smooth muscle cells were intermingled with foam cells or tended to form a cap at the top of lesion in *Apoe*$^{-/-}$ mice at 10–15 wk of age (23). A marked increase of smooth muscle cell content in the plaques was observed in the FK565-administered group ($p = 0.026$; Fig. 2A, 2E). These results suggested that Nod1 ligand accelerated the progression of advanced atherosclerotic lesions, with a remarkable increase of macrophage and T cell infiltration in the plaque.

Contribution of Nod1 in nonhematopoietic cells to the increased atherogenesis by Nod1 ligand administration

As mentioned above, the effect of FK565 in atherogenesis was solely mediated by Nod1. Accordingly, to further test whether non–bone marrow-derived cells expressing Nod1 would contribute to the development of atherosclerosis by FK565 administration, we performed bone marrow transplantation experiments at 20 wk of age. All mice received FK565 for four courses. As expected, the atherosclerotic lesions in aortic roots of *Apoe*$^{-/-}$ mice with *Apoe*$^{-/-}$ bone marrow cells were significantly larger than those of *Apoe*$^{-/-}$*Nod1*$^{-/-}$ mice transplanted with *Apoe*$^{-/-}$*Nod1*$^{-/-}$ bone marrow (Fig. 3). Similarly, in chimeric *Apoe*$^{-/-}$ mice with *Apoe*$^{-/-}$ *Nod1*$^{-/-}$ bone marrow cells, the atherosclerotic lesions were significantly larger than those of *Apoe*$^{-/-}$*Nod1*$^{-/-}$ mice transplanted with either *Apoe*$^{-/-}$ or *Apoe*$^{-/-}$*Nod1*$^{-/-}$ bone marrow. Conversely, chimeric *Apoe*$^{-/-}$*Nod1*$^{-/-}$ mice with *Apoe*$^{-/-}$ bone marrow cells had significantly smaller atherosclerotic lesions than did *Apoe*$^{-/-}$ mice transplanted with either *Apoe*$^{-/-}$ or *Apoe*$^{-/-}$*Nod1*$^{-/-}$ bone marrow (Fig. 3). The data for total aortic plaque formation showed the same trends as did the data for aortic root lesion area discussed above (data not shown). These results indicated that non–bone marrow-derived cells had a pivotal role in acceleration of atherosclerosis induced by Nod1.

Ccl5 is a key chemokine in atherogenesis induced by orally administered Nod1 agonist

To explore the mechanisms underlying the progression of atherosclerosis provoked by Nod1 ligand stimulation, we performed microarray gene expression profiling of the aortic roots of 9-wk-old *Apoe*$^{-/-}$ mice with or without four courses of FK565 administration. Comparative analysis revealed that 1777 genes were up-

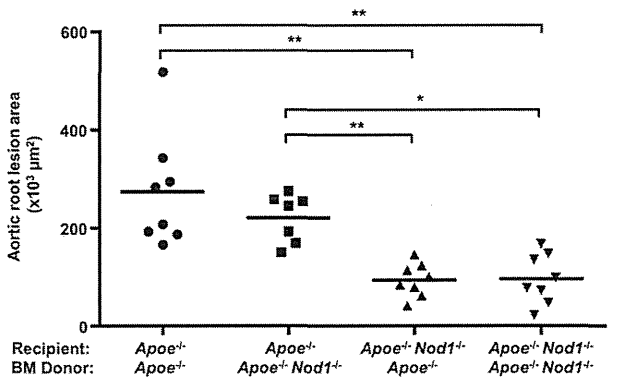

FIGURE 3. Acceleration of atherosclerosis by FK565 depends on Nod1 in nonhematopoietic cells. Quantification of atherosclerotic lesion areas of aortic roots in *Apoe*$^{-/-}$ and *Apoe*$^{-/-}$*Nod1*$^{-/-}$ 20-wk-old mice underwent bone marrow (BM) reconstitution with BM from *Apoe*$^{-/-}$ or *Apoe*$^{-/-}$ *Nod1*$^{-/-}$ donors. All mice were orally administered FK565 (50 μg once a day, 2 d/wk) from 16 to 19 wk of age and fed a chow diet. Bars represent means (n = 7–8/group). *$p < 0.05$, **$p < 0.01$ (Tukey–Kramer honestly significant difference test).

regulated in the aortic roots of FK565-administered mice compared with those of nonadministered mice (Fig. 4A). We also analyzed gene expression in 6-wk-old *Apoe*$^{-/-}$ mice after only one course of FK565 administration, when there was weak accumulation of macrophages in the lesions, which was recognized as the initial stage of atherosclerosis (23) (data not shown). The analysis revealed that 1401 genes were upregulated by one course of FK565 administration, and 100 genes were consistently upregulated by FK565 administration in both time points, indicating that the 100 genes contributed to the initial and early stages of atherosclerosis induced by Nod1 agonist. A gene ontology analysis of the 100 genes showed that a number of biological process terms were associated with immune response (Supplemental Table II). Therefore, we focused on chemokine/cytokine genes. As expected, we identified a number of chemokine/cytokine genes known to be linked to atherosclerosis. The genes upregulated by FK565 in 6-wk-old *Apoe*$^{-/-}$ mice included *Ccl4*, *Ccl5*, *Ccl8*, *Cxcl16*, and *Il2rb*, which are involved in recruitment and activation of macrophage and lymphocyte. In contrast, in 9-wk-old *Apoe*$^{-/-}$ mice, genes associated with recruitment and activation of inflammatory cells, including chemokine/chemokine receptor genes (*Cx3cl1*, *Ccl3*, *Ccl5*, *Ccl8*, *Cxcl1*, *Cxcl12*, *Cxcl16*, *Ccr2*, *Ccr5*, *Cxcr3*, and *Cxcr6*) and IL genes (*Il1b* and *Il6*) were upregulated. In both time points, we observed that three genes were elevated >2-fold (Fig. 4B). To validate the microarray data, we compared expression levels by real-time RT-PCR of these three genes in *Apoe*$^{-/-}$ mice with or without FK565 administration after both one and four courses and found that only one gene, *Ccl5*, also known as RANTES, was significantly upregulated by FK565 administration at both time points (Fig. 4C). Immunore-

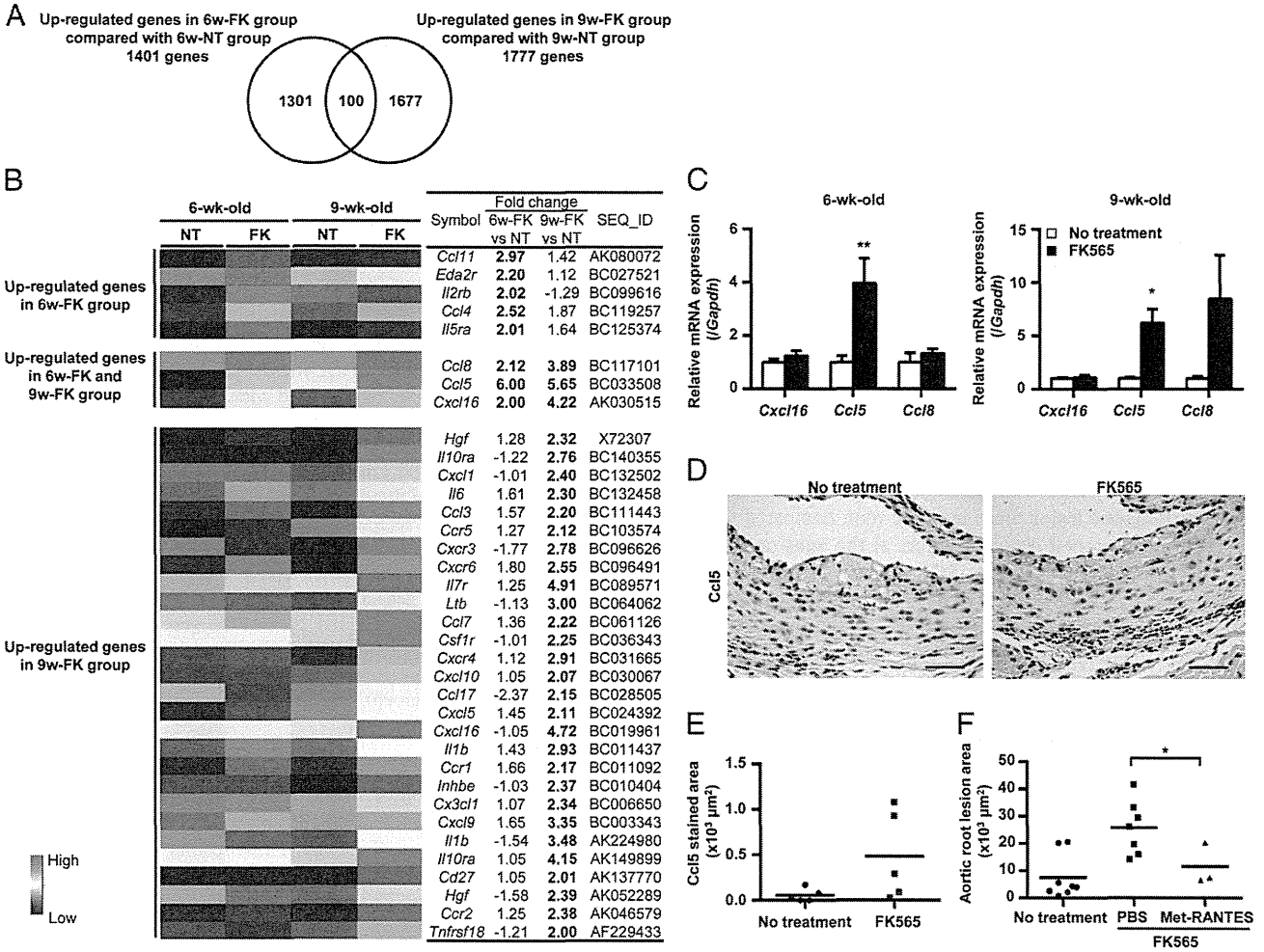

FIGURE 4. Effect of Ccl5 on atherogenesis induced by oral administration of FK565. In microarray analysis (**A** and **B**), total RNA extracted from the aortic roots in *Apoe*$^{-/-}$ mice with or without FK565 administration (FK and NT, respectively) at the age of 6 and 9 wk (6w and 9w, respectively) is shown. Each experiment sample contained three aortic roots from three mice, and two experiments were performed in each group. (A) Venn diagram of upregulated genes in the aortic roots of FK565-administered mice at 6 and/or 9 wk of age. (B) Gene expression ratio and heat map analysis of cytokine/chemokine genes expressed 2-fold higher in FK565-administered *Apoe*$^{-/-}$ mice than in nonadministered *Apoe*$^{-/-}$ mice at 6 or 9 wk of age. Each column represents the mean of the expression levels in each group of replicates. As shown on the color bar, red and blue indicate high and low expressions, respectively. Gene symbols, fold changes in each comparison, and GenBank accession numbers are presented in the *right columns*. Fold changes in bold refer to upregulation >2-fold in each comparison. Data were deposited in Gene Expression Omnibus (http://www.ncbi.nlm.nih.gov/geo/) under accession number GSE48947. (**C**) RT-PCR analysis of *Cxcl16*, *Ccl5*, and *Ccl8* genes in aortic roots of *Apoe*$^{-/-}$ mice with or without FK565 administration at the age of 6 and 9 wk. Gene expression was normalized to expression of *Gapdh*. Relative expression levels to the values observed in aortic root from nonadministered *Apoe*$^{-/-}$ mice are presented as mean ± SEM (n = 5/group). (**D** and **E**) Representative microphotographs (D) and the quantification (E) of positive-stained areas for Ccl5 in aortic roots of *Apoe*$^{-/-}$ mice with or without FK565 administration at 9 wk of age. Scale bars, 50 μm (D). Bars represent means (n = 5/group) (E). (**F**) Quantitative comparison of atherosclerotic lesion areas of aortic roots in FK565-administered *Apoe*$^{-/-}$ mice with i.p. injection of PBS or Met-RANTES before every FK565 administration. Data of nonadministered *Apoe*$^{-/-}$ mice are presented as a control. Bars represent means (n = 3–8/group). *$p < 0.05$, **$p < 0.01$ (Student t test).

activity for Ccl5 was localized in the intimal areas (Fig. 4D), and Nod1 ligands slightly increased Ccl5 levels in the lesions of *Apoe*$^{-/-}$ mice, but without a statistically significant difference (Fig. 4E). To determine a role of Ccl5 in the atherosclerosis progression exerted by Nod1 activation, we investigated whether injection of a Ccl5 antagonist, Met-RANTES, could inhibit the acceleration of atherosclerosis in FK565-administered *Apoe*$^{-/-}$ mice. As expected, Met-RANTES–treated mice showed a significant decrease of atherosclerotic lesion area in aortic root, compared with PBS-treated mice (Fig. 4F), and they had a similar volume of plaques in aortic roots of *Apoe*$^{-/-}$ mice without FK565 administration. These results suggested that Ccl5 plays a crucial role in the acceleration of atherosclerosis induced by FK565.

To determine which cell type frequencies, macrophages or T cells, were altered after Met-RANTES administration, we performed immunohistochemical studies in aortic roots of FK565-administered mice with or without Met-RANTES administration. Both MOMA-2$^+$ macrophages and CD3$^+$ T cells in atherosclerotic lesions significantly decreased after Met-RANTES administration, suggesting that Ccl5 contributes to accumulation of both cell types in the atherosclerotic lesions (Supplemental Fig. 2A, 2B).

Nod1 deficiency reduces atherosclerotic lesion and Ccl5 *gene expression in aortic roots*

To determine whether Nod1 signaling pathway contributes to the early step of atherosclerosis, we studied *Apoe*$^{-/-}$ and *Apoe*$^{-/-}$ *Nod1*$^{-/-}$ male mice at the ages of 9, 12, 20, and 40 wk. *Apoe*$^{-/-}$ *Nod1*$^{-/-}$ mice showed modest elevations of serum cholesterol and triglyceride levels compared with those in *Apoe*$^{-/-}$ mice, but there were no significant differences (Supplemental Table I). Additionally, no difference was observed in the fasting blood glucose levels, serum insulin levels, or homeostasis model assessment of insulin resistance values between *Apoe*$^{-/-}$ and *Apoe*$^{-/-}$*Nod1*$^{-/-}$ mice at 20 wk of age (data not shown). Nonetheless, *Apoe*$^{-/-}$*Nod1*$^{-/-}$ mice showed 43, 63, and 26% decreases of atherosclerotic lesion areas in aortic root, compared with those in their age-matched *Apoe*$^{-/-}$ mice, at the ages of 12, 20, and 40 wk, respectively (Fig. 5A, 5C). By analysis of aortic lesion areas, *Apoe*$^{-/-}$ and *Apoe*$^{-/-}$*Nod1*$^{-/-}$ mice had plaques from 20 wk of age, and they had similar distribution patterns of plaques, with the highest density occurring in the lesser curvature of the aortic arch at 40 wk of age (Fig. 5B). However, plaque formation areas in aortas were significantly reduced (54 and 25%) by Nod1 deficiency at the age of 20 and 40 wk, respectively (Fig. 5B, 5D). These results demonstrated that Nod1 deficiency not only attenuated early atherogenesis but also decelerated the progression of atherosclerosis.

To determine the cellular mechanism for the decelerated atherogenesis by Nod1 deficiency, we analyzed the cell composition of atherosclerotic lesions of *Apoe*$^{-/-}$ mice and *Apoe*$^{-/-}$*Nod1*$^{-/-}$ mice by immunohistochemical studies. The areas for MOMA-2$^+$ macrophages or α-SMA$^+$ smooth muscle cells as well as the numbers of CD3$^+$ T cells or NIMP-R14$^+$ neutrophils in atherosclerotic lesions of *Apoe*$^{-/-}$*Nod1*$^{-/-}$ mice were smaller than those in *Apoe*$^{-/-}$ mice, but the differences were not statistically significant (Supplemental Fig. 2C–F).

In microarray and RT-PCR analyses, Nod1 ligands increased *Ccl5* mRNA levels in aortic root of *Apoe*$^{-/-}$ mice compared with nonadministered mice (Fig. 4B, 4C). *Ccl5* was predominantly upregulated in early plaques (24) and is considered to be important in early lesion formation. Therefore, we examined *Ccl5* gene expression levels in aortic root of *Apoe*$^{-/-}$ and *Apoe*$^{-/-}$*Nod1*$^{-/-}$ mice in early stages of atherosclerosis at 6, 9, 12, and 20 wk of age. At 6–12 wk of age, *Ccl5* mRNA levels in aortic roots of *Apoe*$^{-/-}$*Nod1*$^{-/-}$ mice were lower than those in their age-matched *Apoe*$^{-/-}$ mice, and the difference was statistically significant at 9 wk of age (Fig. 5E). These results suggested that Ccl5 plays crucial roles in the development of atherosclerosis during the early phase induced by Nod1 ligand.

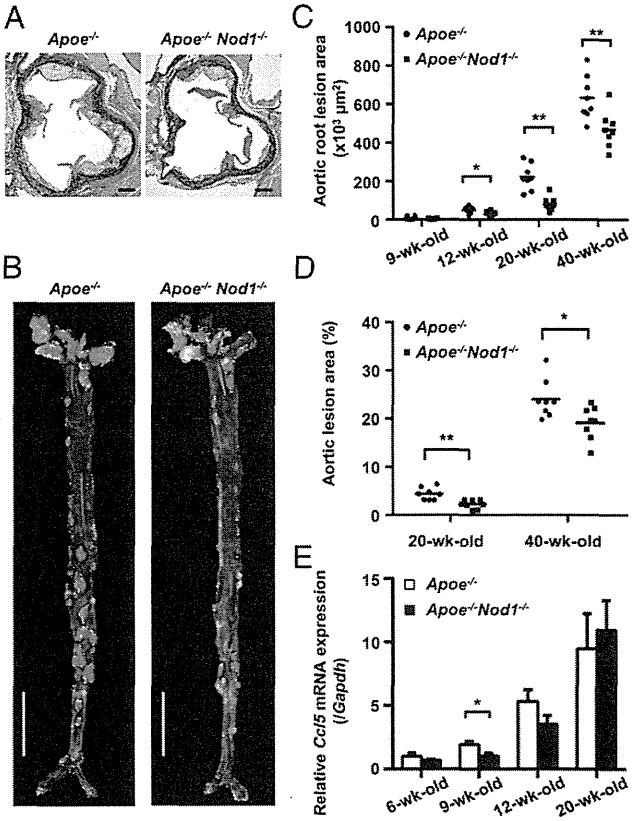

FIGURE 5. Development of atherosclerosis in *Apoe*$^{-/-}$ and *Apoe*$^{-/-}$ *Nod1*$^{-/-}$ mice at 9–40 wk of age without administration of Nod1 ligand. (**A**) Representative aortic roots stained with EVG in *Apoe*$^{-/-}$ or *Apoe*$^{-/-}$ *Nod1*$^{-/-}$ mice at 20 wk of age. Scale bars, 200 μm. (**B**) Representative aortas stained with Sudan IV in *Apoe*$^{-/-}$ or *Apoe*$^{-/-}$*Nod1*$^{-/-}$ mice at 40 wk of age. Scale bars, 500 μm. (**C**) Quantification of atherosclerotic lesion areas of aortic roots in *Apoe*$^{-/-}$ or *Apoe*$^{-/-}$*Nod1*$^{-/-}$ mice at the age of 9, 12, 20, or 40 wk. Bars represent means (n = 6–8/group). (**D**) Quantification of atherosclerotic lesion areas of aortas in *Apoe*$^{-/-}$ or *Apoe*$^{-/-}$*Nod1*$^{-/-}$ mice at the age of 20 or 40 wk. Bars represent means (n = 8/group). (**E**) RT-PCR analysis of *Ccl5* gene in aortic roots of *Apoe*$^{-/-}$ or *Apoe*$^{-/-}$*Nod1*$^{-/-}$ mice at the age of 6, 9, 12, and 20 wk. The gene expression was normalized to expression of *Gapdh*. Relative expression levels to the values observed in aortic root from 6-wk-old *Apoe*$^{-/-}$ mice are presented as mean ± SEM (n = 5/group). *$p < 0.05$, **$p < 0.01$ versus *Apoe*$^{-/-}$ mice at the same age (Student t test).

Discussion

The present study has demonstrated that long-term oral administration of a pure synthetic Nod1 ligand accelerated the development and progression of atherosclerosis in *Apoe*$^{-/-}$ mice, independent of cholesterol or triglyceride levels in blood. Additionally, the complete loss of this receptor significantly decreased the size of atherosclerotic lesions, providing evidence of a solid relationship between NOD1 and atherosclerosis. Previously, only limited studies have shown the effect of NOD1 in the cardiovascular field (25, 26) or the involvement of NOD1 in vascular inflammation induced by *C. pneumoniae* (12). No prior study, however, has directly proven the association between NOD1 and atherosclerosis in vivo.

By transplantation experiments, the major effector cells of the Nod1 ligand were nonhematopoietic cells. This is consistent with the observation that NOD1 in nonhematopoietic cells plays a key role in activation of human endothelial cells, mediated by *C. pneumoniae* (12), the chronic or recurrent infection of which was reported to have a close relationship to the development of atherosclerosis (27). Alternatively, Levin et al. (28) showed that increased lipid intake in *receptor-interacting protein 2* $(Rip2)^{-/-}$ macrophages resulted in increased atherosclerotic lesions in *apolipoprotein* $B^{-/-}$*low-density lipoprotein receptor*$^{-/-}$ mice transplanted with $Rip2^{-/-}$ bone marrow. Myeloid-specific depletion of Nod1 showed no significant difference in plaque formation in our study, and myeloid-specific depletion of Nod2, but not Rip2, showed significant reduction in the lipid-rich necrotic area in *low-density lipoprotein receptor*$^{-/-}$ mice (29). Therefore, it is possible that $Rip2^{-/-}$ macrophages exert their effects mainly through the alteration of lipid metabolism rather than Nod1 or Nod2 signaling pathways.

The marked expression of *Ccl5* mRNA gene in the Nod1-induced atherosclerotic lesions and the inhibitory effect of Met-RANTES on Nod1-induced acceleration of atherosclerosis demonstrated that *Ccl5* expression might be pathophysiologically important for the development and/or advancement of atherosclerosis. Consistent with the previous report that *Ccl5* expression was most marked in early plaque (24), the effect of Nod1 for plaque formation appeared to be dominant at early stage (<12 wk) because there was a marked downregulation of *Ccl5* expression at that stage in $Apoe^{-/-}Nod1^{-/-}$ mice. Ccl5 is a proinflammatory chemokine that regulates the trafficking of leukocytes such as macrophages and Th1 T cells, mediated by activation of the receptors Ccr1, Ccr3, Ccr4, and Ccr5 (30). In atherosclerosis, Ccr5 is known to be involved, not only in the recruitment of mononuclear cell, but also in the modulation of the immune balance (18, 31–33). Similarly, in FK565-administered $Apoe^{-/-}$ mice, Met-RANTES administration attenuated the infiltration of MOMA-2^+ macrophages and $CD3^+$ T cells in atherosclerotic lesions, suggesting that accumulation of both cell types by Ccl5 plays a role in Nod1-induced acceleration of atherosclerosis.

It has been reported that chronic or repeated infection was a strong risk factor for the development and aggravation of atherosclerosis (27, 34–36). However, it was difficult to show direct evidence of existing microorganisms in atherosclerotic plaques. Several studies showed the bacterial PGNs or DNA fragments existing in atherosclerotic plaques (37–39), and the metagenomic analysis of gut microbiome in patients with symptomatic atherosclerotic plaques and healthy controls demonstrated that patient metagenomes were enriched in genes encoding PGN biosynthesis (40). Furthermore, a recent report demonstrated that PGNs from microbiota were detected in systemically circulating blood, and they modulated the innate immune system through Nod1 (41). In the present study, we have demonstrated that Nod1 ligand directly contributed to the development of atherosclerosis. Taken together, systemically circulating PGN fragments from endogenous microbiota may activate Nod1-expressing vascular cells to produce various chemokines, including Ccl5, to promote the accumulation of inflammatory cells in the plaques and eventually accelerate the atherosclerotic formation in vessels. Although endogenous Nod1 ligands are still unknown, it is possible that yet-undetermined endogenous Nod1 ligands contribute to the development of atherosclerosis, because there are several studies that endogenous ligands toward other PRRs such as Tlr2, Tlr4, and Nlrp3 were involved in the acceleration of atherosclerosis (11, 42–45).

A recent study showed that gut flora influenced the nutrient processing and the metabolism in mice, and microbial processing of dietary choline was significantly correlated with atherosclerosis (46). Although it is still controversial whether Nod1 deficiency contributes to alteration of the composition of microflora (47, 48), alteration of the microbiota by Nod1 deficiency might play a role in the decreased development of atherosclerosis in $Apoe^{-/-}$ $Nod1^{-/-}$ mice. Because oral administration of FK565 might influence microbiota in the long-term observation, further investigation is needed on a role of microbiota in the acceleration of atherosclerosis through Nod1 activation.

In the previous studies, endogenous and synthetic ligands for Tlr2 and Tlr4 influenced the formation of atherosclerosis in addition to Nod1 (7, 9, 49). We found that Nod1 deficiency significantly reduced plaque formation by 50% in the aortas of 20-wk-old $Apoe^{-/-}$ mice, indicating that the contribution of Nod1 on atherogenesis is as strong as those of Tlr2 and Tlr4 suggested by the previous study (49). Interestingly, the effect of Nod1 for plaque formation seemed to be dominant at early stage (<12 wk) as shown by marked downregulation of Ccl5 expression in $Nod1^{-/-}$ mice. Hence, it is possible that the ligand-specific effects of innate immune-mediated atherosclerosis formation might exist, and various types of ligands from microbiota would independently or synergistically work together for the development of atherosclerosis.

In conclusion, Nod1 activation plays one of the key roles in the development and progression of atherosclerosis. Further comprehensive studies on the innate immune ligand-specific contribution are necessary to understand the pathogenesis of atherosclerosis.

Acknowledgments

We are thankful to H. Fujii and C. Arimatsu for technical assistance, J. Kishimoto for statistical analyses, and Y. Nakashima for planning advice.

Disclosures

The authors have no financial conflicts of interest.

References

1. Ross, R. 1999. Atherosclerosis—an inflammatory disease. *N. Engl. J. Med.* 340: 115–126.
2. Packard, R. R., E. Maganto-García, I. Gotsman, I. Tabas, P. Libby, and A. H. Lichtman. 2008. $CD11c^+$ dendritic cells maintain antigen processing, presentation capabilities, and $CD4^+$ T-cell priming efficacy under hypercholesterolemic conditions associated with atherosclerosis. *Circ. Res.* 103: 965–973.
3. Zhou, X., A. Nicoletti, R. Elhage, and G. K. Hansson. 2000. Transfer of $CD4^+$ T cells aggravates atherosclerosis in immunodeficient apolipoprotein E knockout mice. *Circulation* 102: 2919–2922.
4. Edfeldt, K., J. Swedenborg, G. K. Hansson, and Z. Q. Yan. 2002. Expression of Toll-like receptors in human atherosclerotic lesions: a possible pathway for plaque activation. *Circulation* 105: 1158–1161.
5. Naiki, Y., R. Sorrentino, M. H. Wong, K. S. Michelsen, K. Shimada, S. Chen, A. Yilmaz, A. Slepenkin, N. W. J. Schröder, T. R. Crother, et al. 2008. TLR/MyD88 and liver X receptor α signaling pathways reciprocally control *Chlamydia pneumoniae*-induced acceleration of atherosclerosis. *J. Immunol.* 181: 7176–7185.
6. Gibson, F. C., III, C. Hong, H. H. Chou, H. Yumoto, J. Chen, E. Lien, J. Wong, and C. A. Genco. 2004. Innate immune recognition of invasive bacteria accelerates atherosclerosis in apolipoprotein E-deficient mice. *Circulation* 109: 2801–2806.
7. Mullick, A. E., P. S. Tobias, and L. K. Curtiss. 2005. Modulation of atherosclerosis in mice by Toll-like receptor 2. *J. Clin. Invest.* 115: 3149–3156.
8. Takeuchi, O., and S. Akira. 2010. Pattern recognition receptors and inflammation. *Cell* 140: 805–820.
9. Michelsen, K. S., M. H. Wong, P. K. Shah, W. Zhang, J. Yano, T. M. Doherty, S. Akira, T. B. Rajavashisth, and M. Arditi. 2004. Lack of Toll-like receptor 4 or myeloid differentiation factor 88 reduces atherosclerosis and alters plaque phenotype in mice deficient in apolipoprotein E. *Proc. Natl. Acad. Sci. USA* 101: 10679–10684.
10. Björkbacka, H., V. V. Kunjathoor, K. J. Moore, S. Koehn, C. M. Ordija, M. A. Lee, T. Means, K. Halmen, A. D. Luster, D. T. Golenbock, and M. W. Freeman. 2004. Reduced atherosclerosis in MyD88-null mice links elevated serum cholesterol levels to activation of innate immunity signaling pathways. *Nat. Med.* 10: 416–421.
11. Duewell, P., H. Kono, K. J. Rayner, C. M. Sirois, G. Vladimer, F. G. Bauernfeind, G. S. Abela, L. Franchi, G. Nuñez, M. Schnurr, et al. 2010.

NLRP3 inflammasomes are required for atherogenesis and activated by cholesterol crystals. *Nature* 464: 1357–1361.
12. Opitz, B., S. Förster, A. C. Hocke, M. Maass, B. Schmeck, S. Hippenstiel, N. Suttorp, and M. Krüll. 2005. Nod1-mediated endothelial cell activation by *Chlamydophila pneumoniae*. *Circ. Res.* 96: 319–326.
13. Girardin, S. E., I. G. Boneca, L. A. M. Carneiro, A. Antignac, M. Jéhanno, J. Viala, K. Tedin, M. K. Taha, A. Labigne, U. Zähringer, et al. 2003. Nod1 detects a unique muropeptide from gram-negative bacterial peptidoglycan. *Science* 300: 1584–1587.
14. Inohara, N., T. Koseki, L. del Peso, Y. Hu, C. Yee, S. Chen, R. Carrio, J. Merino, D. Liu, J. Ni, and G. Núñez. 1999. Nod1, an Apaf-1-like activator of caspase-9 and nuclear factor-κB. *J. Biol. Chem.* 274: 14560–14567.
15. Bertin, J., W. J. Nir, C. M. Fischer, O. V. Tayber, P. R. Errada, J. R. Grant, J. J. Keilty, M. L. Gosselin, K. E. Robison, G. H. Wong, et al. 1999. Human CARD4 protein is a novel CED-4/Apaf-1 cell death family member that activates NF-κB. *J. Biol. Chem.* 274: 12955–12958.
16. Nishio, H., S. Kanno, S. Onoyama, K. Ikeda, T. Tanaka, K. Kusuhara, Y. Fujimoto, K. Fukase, K. Sueishi, and T. Hara. 2011. Nod1 ligands induce site-specific vascular inflammation. *Arterioscler. Thromb. Vasc. Biol.* 31: 1093–1099.
17. Shigeoka, A. A., A. Kambo, J. C. Mathison, A. J. King, W. F. Hall, J. da Silva Correia, R. J. Ulevitch, and D. B. McKay. 2010. Nod1 and Nod2 are expressed in human and murine renal tubular epithelial cells and participate in renal ischemia reperfusion injury. *J. Immunol.* 184: 2297–2304.
18. Veillard, N. R., B. Kwak, G. Pelli, F. Mulhaupt, R. W. James, A. E. Proudfoot, and F. Mach. 2004. Antagonism of RANTES receptors reduces atherosclerotic plaque formation in mice. *Circ. Res.* 94: 253–261.
19. Goossens, P., M. J. Gijbels, A. Zernecke, W. Eijgelaar, M. N. Vergouwe, I. van der Made, J. Vanderlocht, L. Beckers, W. A. Buurman, M. J. Daemen, et al. 2010. Myeloid type I interferon signaling promotes atherosclerosis by stimulating macrophage recruitment to lesions. *Cell Metab.* 12: 142–153.
20. Liou, J. T., C. C. Mao, D. Ching-Wah Sum, F. C. Liu, Y. S. Lai, J. C. Li, and Y. J. Day. 2013. Peritoneal administration of Met-RANTES attenuates inflammatory and nociceptive responses in a murine neuropathic pain model. *J. Pain* 14: 24–35.
21. Reikvam, D. H., A. Erofeev, A. Sandvik, V. Grcic, F. L. Jahnsen, P. Gaustad, K. D. McCoy, A. J. Macpherson, L. A. Meza-Zepeda, and F. E. Johansen. 2011. Depletion of murine intestinal microbiota: effects on gut mucosa and epithelial gene expression. *PLoS ONE* 6: e17996.
22. Paigen, B., A. Morrow, P. A. Holmes, D. Mitchell, and R. A. Williams. 1987. Quantitative assessment of atherosclerotic lesions in mice. *Atherosclerosis* 68: 231–240.
23. Nakashima, Y., A. S. Plump, E. W. Raines, J. L. Breslow, and R. Ross. 1994. ApoE-deficient mice develop lesions of all phases of atherosclerosis throughout the arterial tree. *Arterioscler. Thromb.* 14: 133–140.
24. Lutgens, E., B. Faber, K. Schapira, C. T. Evelo, R. van Haaften, S. Heeneman, K. B. Cleutjens, A. P. Bijnens, L. Beckers, J. G. Porter, et al. 2005. Gene profiling in atherosclerosis reveals a key role for small inducible cytokines: validation using a novel monocyte chemoattractant protein monoclonal antibody. *Circulation* 111: 3443–3452.
25. Cartwright, N., O. Murch, S. K. McMaster, M. J. Paul-Clark, D. A. van Heel, B. Ryffel, V. F. Quesniaux, T. W. Evans, C. Thiemermann, and J. A. Mitchell. 2007. Selective NOD1 agonists cause shock and organ injury/dysfunction in vivo. *Am. J. Respir. Crit. Care Med.* 175: 595–603.
26. Moreno, L., S. K. McMaster, T. Gatheral, L. K. Bailey, L. S. Harrington, N. Cartwright, P. C. Armstrong, T. D. Warner, M. Paul-Clark, and J. A. Mitchell. 2010. Nucleotide oligomerization domain 1 is a dominant pathway for NOS2 induction in vascular smooth muscle cells: comparison with Toll-like receptor 4 responses in macrophages. *Br. J. Pharmacol.* 160: 1997–2007.
27. Maass, M., C. Bartels, P. M. Engel, U. Mamat, and H. H. Sievers. 1998. Endovascular presence of viable *Chlamydia pneumoniae* is a common phenomenon in coronary artery disease. *J. Am. Coll. Cardiol.* 31: 827–832.
28. Levin, M. C., P. Jirholt, A. Wramstedt, M. E. Johansson, A. M. Lundberg, M. G. Trajkovska, M. Ståhlman, P. Fogelstrand, M. Brisslert, L. Fogelstrand, et al. 2011. *Rip2* deficiency leads to increased atherosclerosis despite decreased inflammation. *Circ. Res.* 109: 1210–1218.
29. Johansson, M. E., X. Y. Zhang, K. Edfeldt, A. M. Lundberg, M. C. Levin, J. Borén, W. Li, X. M. Yuan, L. Folkersen, P. Eriksson, et al. 2014. Innate immune receptor NOD2 promotes vascular inflammation and formation of lipid-rich necrotic cores in hypercholesterolemic mice. *Eur. J. Immunol.* 44: 3081–3092.
30. Appay, V., and S. L. Rowland-Jones. 2001. RANTES: a versatile and controversial chemokine. *Trends Immunol.* 22: 83–87.
31. Weber, C., and H. Noels. 2011. Atherosclerosis: current pathogenesis and therapeutic options. *Nat. Med.* 17: 1410–1422.
32. Braunersreuther, V., A. Zernecke, C. Arnaud, E. A. Liehn, S. Steffens, E. Shagdarsuren, K. Bidzhekov, F. Burger, G. Pelli, B. Luckow, et al. 2007. Ccr5 but not Ccr1 deficiency reduces development of diet-induced atherosclerosis in mice. *Arterioscler. Thromb. Vasc. Biol.* 27: 373–379.
33. Potteaux, S., C. Combadière, B. Esposito, C. Lecureuil, H. Ait-Oufella, R. Merval, P. Ardouin, A. Tedgui, and Z. Mallat. 2006. Role of bone marrow-derived CC-chemokine receptor 5 in the development of atherosclerosis of low-density lipoprotein receptor knockout mice. *Arterioscler. Thromb. Vasc. Biol.* 26: 1858–1863.
34. Saikku, P., M. Leinonen, L. Tenkanen, E. Linnanmäki, M. R. Ekman, V. Manninen, M. Mänttäri, M. H. Frick, and J. K. Huttunen. 1992. Chronic *Chlamydia pneumoniae* infection as a risk factor for coronary heart disease in the Helsinki Heart Study. *Ann. Intern. Med.* 116: 273–278.
35. Chiu, B., E. Viira, W. Tucker, and I. W. Fong. 1997. *Chlamydia pneumoniae*, cytomegalovirus, and herpes simplex virus in atherosclerosis of the carotid artery. *Circulation* 96: 2144–2148.
36. Kiechl, S., G. Egger, M. Mayr, C. J. Wiedermann, E. Bonora, F. Oberhollenzer, M. Muggeo, Q. Xu, G. Wick, W. Poewe, and J. Willeit. 2001. Chronic infections and the risk of carotid atherosclerosis: prospective results from a large population study. *Circulation* 103: 1064–1070.
37. Laman, J. D., A. H. Schoneveld, F. L. Moll, M. van Meurs, and G. Pasterkamp. 2002. Significance of peptidoglycan, a proinflammatory bacterial antigen in atherosclerotic arteries and its association with vulnerable plaques. *Am. J. Cardiol.* 90: 119–123.
38. Ott, S. J., N. E. El Mokhtari, M. Musfeldt, S. Hellmig, S. Freitag, A. Rehman, T. Kühbacher, S. Nikolaus, P. Namsolleck, M. Blaut, et al. 2006. Detection of diverse bacterial signatures in atherosclerotic lesions of patients with coronary heart disease. *Circulation* 113: 929–937.
39. Koren, O., A. Spor, J. Felin, F. Fåk, J. Stombaugh, V. Tremaroli, C. J. Behre, R. Knight, B. Fagerberg, R. E. Ley, and F. Bäckhed. 2011. Human oral, gut, and plaque microbiota in patients with atherosclerosis. *Proc. Natl. Acad. Sci. USA* 108(Suppl. 1): 4592–4598.
40. Karlsson, F. H., F. Fåk, I. Nookaew, V. Tremaroli, B. Fagerberg, D. Petranovic, F. Bäckhed, and J. Nielsen. 2012. Symptomatic atherosclerosis is associated with an altered gut metagenome. *Nat. Commun.* 3: 1245.
41. Clarke, T. B., K. M. Davis, E. S. Lysenko, A. Y. Zhou, Y. Yu, and J. N. Weiser. 2010. Recognition of peptidoglycan from the microbiota by Nod1 enhances systemic innate immunity. *Nat. Med.* 16: 228–231.
42. Ohashi, K., V. Burkart, S. Flohé, and H. Kolb. 2000. Cutting edge: heat shock protein 60 is a putative endogenous ligand of the toll-like receptor-4 complex. *J. Immunol.* 164: 558–561.
43. Kanwar, R. K., J. R. Kanwar, D. Wang, D. J. Ormrod, and G. W. Krissansen. 2001. Temporal expression of heat shock proteins 60 and 70 at lesion-prone sites during atherogenesis in ApoE-deficient mice. *Arterioscler. Thromb. Vasc. Biol.* 21: 1991–1997.
44. Smiley, S. T., J. A. King, and W. W. Hancock. 2001. Fibrinogen stimulates macrophage chemokine secretion through Toll-like receptor 4. *J. Immunol.* 167: 2887–2894.
45. Okamura, Y., M. Watari, E. S. Jerud, D. W. Young, S. T. Ishizaka, J. Rose, J. C. Chow, and J. F. Strauss, III. 2001. The extra domain A of fibronectin activates Toll-like receptor 4. *J. Biol. Chem.* 276: 10229–10233.
46. Koeth, R. A., Z. Wang, B. S. Levison, J. A. Buffa, E. Org, B. T. Sheehy, E. B. Britt, X. Fu, Y. Wu, L. Li, et al. 2013. Intestinal microbiota metabolism of L-carnitine, a nutrient in red meat, promotes atherosclerosis. *Nat. Med.* 19: 576–585.
47. Bouskra, D., C. Brézillon, M. Bérard, C. Werts, R. Varona, I. G. Boneca, and G. Eberl. 2008. Lymphoid tissue genesis induced by commensals through NOD1 regulates intestinal homeostasis. *Nature* 456: 507–510.
48. Robertson, S. J., J. Y. Zhou, K. Geddes, S. J. Rubino, J. H. Cho, S. E. Girardin, and D. J. Philpott. 2013. Nod1 and Nod2 signaling does not alter the composition of intestinal bacterial communities at homeostasis. *Gut Microbes* 4: 222–231.
49. Higashimori, M., J. B. Tatro, K. J. Moore, M. E. Mendelsohn, J. B. Galper, and D. Beasley. 2011. Role of Toll-like receptor 4 in intimal foam cell accumulation in apolipoprotein E-deficient mice. *Arterioscler. Thromb. Vasc. Biol.* 31: 50–57.